

ASC Report No. 6/2010

Convergence of Some Adaptive FEM-BEM Coupling

Markus Aurada, Michael Feischl, Dirk Praetorius

Institute for Analysis and Scientific Computing
Vienna University of Technology — TU Wien
www.asc.tuwien.ac.at ISBN 978-3-902627-03-2

Most recent ASC Reports

- 5/2010 *Marcus Page, Dirk Praetorius*
Convergence of Adaptive FEM for some Elliptic Obstacle Problem
- 4/2010 *Ansgar Jüngel, Josipa-Pina Milišić*
A Simplified Quantum Energy-Transport Model for Semiconductors
- 3/2010 *Georg Kitzhofer, Othmar Koch, Gernot Pulverer, Christa Simon, Ewa Weinmüller*
The New MATLAB Code bvpsuite for the Solution of Singular Implicit BVPs
- 2/2010 *Maike Löhndorf, Jens Markus Melenk*
Wavenumber-explicit hp-BEM for High Frequency Scattering
- 1/2010 *Jens Markus Melenk*
Mapping Properties of Combined Field Helmholtz Boundary Integral Operators
- 49/2009 *Markus Aurada, Jens Markus Melenk, Dirk Praetorius*
Mixed Conforming Elements for the Large-Body Limit in Micromagnetics
- 48/2009 *Irene Reichl, Winfried Auzinger, Heinz-Bodo Schmiedmayer, Ewa Weinmüller*
Reconstructing the Knee Joint Mechanism from Kinematic Data
- 47/2009 *Irena Rachůnková, Svatoslav Staněk, Ewa Weinmüller, Michael Zenz*
Neumann Problems with Time Singularities
- 46/2009 *Kazuo Aoki, Ansgar Jüngel, Peter A. Markovich*
Small Velocity and finite Temperature Variations in Kinetic Relaxation Models
- 45/2009 *Ansgar Jüngel, Jan-Frederik Mennemann*
Time-dependent Simulations of Multidimensional Quantum Waveguides Using a Time-Splitting Spectral method

Institute for Analysis and Scientific Computing
Vienna University of Technology
Wiedner Hauptstraße 8–10
1040 Wien, Austria

E-Mail: admin@asc.tuwien.ac.at
WWW: <http://www.asc.tuwien.ac.at>
FAX: +43-1-58801-10196

ISBN 978-3-902627-03-2

© Alle Rechte vorbehalten. Nachdruck nur mit Genehmigung des Autors.



CONVERGENCE OF SOME ADAPTIVE FEM-BEM COUPLING

M. AURADA, M. FEISCHL, AND D. PRAETORIUS

ABSTRACT. We consider the symmetric FEM-BEM coupling for the numerical solution of a (nonlinear) interface problem for the 2D Laplacian. We introduce some new a posteriori error estimators based on the $(h - h/2)$ -error estimation strategy. In particular, these include the approximation error for the boundary data, which allows to work with discrete boundary integral operators only. Using the concept of estimator reduction, we prove that the proposed adaptive algorithm is convergent in the sense that it drives the underlying error estimator to zero. Numerical experiments underline the reliability and efficiency of the considered adaptive mesh-refinement.

1. INTRODUCTION & OVERVIEW

The $(h - h/2)$ -error estimation strategy is a well-known technique for the a posteriori estimation of the error in the energy norm $\| \| u - u_\ell \| \|$; see [20] in the context of ordinary differential equations, and the overview article of Bank [5] or the monograph [1, Chapter 5] in the context of the finite element method: Let \mathcal{X}_ℓ be a discrete subspace of the energy space \mathcal{H} and let $\widehat{\mathcal{X}}_\ell$ be its uniform refinement. With the corresponding Galerkin solution \mathbf{U}_ℓ and $\widehat{\mathbf{U}}_\ell$, the $(h - h/2)$ -error estimator

$$(1) \quad \eta_\ell := \| \| \widehat{\mathbf{U}}_\ell - \mathbf{U}_\ell \| \|$$

is a computable quantity [13] which can be used to estimate the error $\| \| \mathbf{u} - \mathbf{U}_\ell \| \|$, where $\mathbf{u} \in \mathcal{H}$ denotes the exact solution and where $\| \| \cdot \| \|$ denotes the energy norm on \mathcal{H} .

For finite element methods (FEM), the energy norm, e.g., $\| \| \cdot \| \| = \|\nabla(\cdot)\|_{L^2(\Omega)}$ provides local information, which elements of the underlying mesh should be refined to decrease the error effectively. For boundary element methods (BEM), the energy norm $\| \| \cdot \| \|$ is (equivalent to) a fractional order Sobolev norm and typically does not provide a direct information, where the underlying mesh should be refined. In [18], localized variants of η_ℓ were introduced. In [15, 16] the equivalence of η_ℓ to hierarchical two-level error estimators from [21, 25] and averaging error estimators from [7, 8, 9] has been analyzed.

Recently [17], convergence of some $(h - h/2)$ -steered adaptive mesh-refinement has been proven for linear model problems in the context of FEM and BEM. In [3, 4], this result has been generalized to averaging type error estimators and perturbed Galerkin schemes. The latter is important in the context of BEM, since the involved integral operators can, in general, only be evaluated for discrete functions.

In this work, we introduce some $(h - h/2)$ -type error estimators for the coupling of FEM and BEM. As model problem, we consider an interface problem in two dimensions with a nonlinear inhomogeneous partial differential equation (PDE) in the interior domain and a linear homogeneous PDE in the exterior domain. We apply a symmetric coupling method [12,

11] and the lowest-order Galerkin scheme to obtain a (nonlinear) system of coupled FEM-BEM equations. For linear problems, the ideas from [15, 16] can be used to prove that the introduced error estimators are equivalent to the two-level error estimator from [24].

Using ideas from [4] and in addition to the seminal work [24], we include the approximation of the data to deal with discrete integral operators only. Moreover, [24] proves that a saturation condition

$$(2) \quad \|\mathbf{u} - \mathbf{U}_{\ell+1}\| \leq q \|\mathbf{u} - \mathbf{U}_\ell\|$$

for a sequence \mathbf{U}_ℓ of discrete FEM-BEM solutions and with some uniform constant $0 < q < 1$, implies the reliability of the two-level error estimator. On the other hand, this saturation condition already assumes linear convergence of the discrete solutions obtained from an adaptive mesh-refining algorithm. In our work, we assume that uniform refinement, i.e. the use of $\widehat{\mathbf{U}}_\ell$ instead of $\mathbf{U}_{\ell+1}$ in (2), guarantees a saturation condition. Under this — compared to [24] — much weaker assumption, we prove that the introduced $(h - h/2)$ -error estimator is reliable and efficient up to data approximation terms, which are also controlled a posteriori. Finally, we prove that the usual adaptive algorithm drives the error estimator (and hence the error) to zero. We stress that this is the first convergence result available for adaptive schemes in the context of the FEM-BEM coupling.

The outline of the paper is as follows: In Section 2.1, we formulate our model problem, and the Galerkin formulation is given in Section 2.2–2.3. Section 3.1 collects the properties of the local mesh-refinement used for the numerical analysis. In Section 3.2, we introduce a computable data oscillation term osc_ℓ . We prove that osc_ℓ provides the means to control the error introduced by the data approximation (Proposition 1). In Section 3.3, we state the saturation assumption (36) and prove that the $(h - h/2)$ -error estimator η_ℓ from (1) provides, up to osc_ℓ , a lower and upper bound for the error $\|\mathbf{u} - \mathbf{U}_\ell\|$ (Proposition 6). As mentioned before, the boundary contribution to the energy norm $\|\cdot\|$ cannot be used to steer an adaptive mesh-refinement. In the spirit of [18], we introduce further estimators μ_ℓ and $\tilde{\mu}_\ell$ in Section 3.4, which are equivalent to η_ℓ (Lemma 7) and which can be used to steer an adaptive algorithm. Consequently (Theorem 8), these estimators provide, up to osc_ℓ , lower and upper bounds for the error. Section 4 provides our version of the adaptive algorithm (Algorithm 12) and proves convergence (Theorem 13). The first ingredient of our convergence proof is the observation that adaptive mesh-refinement always leads to a convergent sequence of discrete solutions \mathbf{U}_ℓ , where the limit

$$(3) \quad \mathbf{u}_\infty := \lim_{\ell \rightarrow \infty} \mathbf{U}_\ell,$$

however, does not necessarily coincide with the continuous solution \mathbf{u} (Proposition 10). Second, we show that a generalized variant (53)–(54) of the Dörfler marking [14] implies an estimator reduction estimate of the type

$$(4) \quad \tilde{\varrho}_{\ell+1}^2 \leq \kappa \tilde{\varrho}_\ell^2 + C \|\widehat{\mathbf{U}}_{\ell+1} - \widehat{\mathbf{U}}_\ell\|^2$$

with $\tilde{\varrho}_\ell^2 := \tilde{\mu}_\ell^2 + \text{osc}_\ell^2$ and with certain ℓ -independent constants $0 < \kappa < 1$ and $C > 0$ (Lemma 11). From the a priori convergence (3) of $\widehat{\mathbf{U}}_\ell$ to some limit $\widehat{\mathbf{u}}_\infty$, one may thus conclude convergence $\tilde{\varrho}_\ell \rightarrow 0$ as $\ell \rightarrow \infty$, cf. [3]. Section 5 gives empirical evidence that the proposed adaptive algorithm is much superior to uniform mesh-refinement with respect to both, experimental convergence rate and computational time. Finally, a short appendix

generalizes a result of [11] and proves that, without any further assumptions on the mesh-sizes, each discrete space \mathcal{X}_ℓ admits a unique Galerkin solution \mathbf{U}_ℓ .

2. CONTINUOUS PROBLEM AND GALERKIN FORMULATION

2.1. Model Problem. We consider the nonlinear interface problem

$$(5) \quad \left\{ \begin{array}{ll} -\operatorname{div}(A\nabla u^{\text{int}}) = f & \text{in } \Omega^{\text{int}} := \Omega, \\ -\Delta u^{\text{ext}} = 0 & \text{in } \Omega^{\text{ext}} := \mathbb{R}^2 \setminus \overline{\Omega}, \\ u^{\text{int}} - u^{\text{ext}} = u_0 & \text{on } \Gamma, \\ (A\nabla u^{\text{int}} - \nabla u^{\text{ext}}) \cdot n = \phi_0 & \text{on } \Gamma, \\ u^{\text{ext}}(x) = \mathcal{O}(\log|x|) & \text{as } |x| \rightarrow \infty. \end{array} \right.$$

Here, Ω is a bounded Lipschitz domain in \mathbb{R}^2 with boundary $\Gamma := \partial\Omega$ and outer unit normal vector n . The given data satisfy $f \in L^2(\Omega)$, $u_0 \in H^{1/2}(\Gamma)$, and $\phi_0 \in H^{-1/2}(\Gamma)$. We recall that $\tilde{H}^{-1}(\Omega)$ is the dual space of $H^1(\Omega)$ with respect to the $L^2(\Omega)$ -scalar product. The space $H^{1/2}(\Gamma)$ is precisely the space of all traces of functions from $H^1(\Omega)$, and $H^{-1/2}(\Gamma)$ is the dual of $H^{1/2}(\Gamma)$ with respect to the $L^2(\Gamma)$ -scalar product.

As usual, (5) is understood in the weak sense, and the sought solutions satisfy $u^{\text{int}} \in H^1(\Omega)$ and $u^{\text{ext}} \in H_{loc}^1(\Omega^{\text{ext}}) = \{v : \Omega^{\text{ext}} \rightarrow \mathbb{R} : \forall K \subset \Omega^{\text{ext}} \text{ compact } v \in H^1(K)\}$. The (possibly nonlinear) operator $A : L^2(\Omega)^2 \rightarrow L^2(\Omega)^2$ is strongly monotone and Lipschitz continuous, i.e. there holds

$$(6) \quad \left\{ \begin{array}{l} C_{\text{mon}} \|\nabla v - \nabla w\|_{L^2(\Omega)}^2 \leq \langle A\nabla v - A\nabla w, \nabla v - \nabla w \rangle_\Omega, \\ \|\nabla v - \nabla w\|_{L^2(\Omega)} \leq C_{\text{lip}} \|\nabla v - \nabla w\|_{L^2(\Omega)}, \end{array} \right.$$

for all $v, w \in H^1(\Omega)$.

Problem (5) is equivalently stated via the symmetric FEM-BEM coupling, cf. e.g. [11, Theorem 1]: Find $(u, \phi) \in \mathcal{H} := H^1(\Omega) \times H^{-1/2}(\Gamma)$ such that

$$(7) \quad \left\{ \begin{array}{l} \langle A\nabla u, \nabla v \rangle_\Omega + \langle \mathfrak{W}u + (\mathfrak{K}' - \frac{1}{2})\phi, v \rangle_\Gamma = \langle f, v \rangle_\Omega + \langle \phi_0 + \mathfrak{W}u_0, v \rangle_\Gamma, \\ \langle \psi, \mathfrak{V}\phi - (\mathfrak{K} - \frac{1}{2})u \rangle_\Gamma = -\langle \psi, (\mathfrak{K} - \frac{1}{2})u_0 \rangle_\Gamma, \end{array} \right.$$

for all $(v, \psi) \in \mathcal{H}$. Here, \mathfrak{V} denotes the simple-layer potential, \mathfrak{K} denotes the double-layer potential with adjoint \mathfrak{K}' , and \mathfrak{W} denotes the hypersingular integral operator. With

$$(8) \quad G(z) := -\frac{1}{2\pi} \log|z| \quad \text{for } z \in \mathbb{R}^2 \setminus \{0\}$$

the fundamental solution of the 2D Laplacian, these integral operators formally read for $x \in \Gamma$ as follows,

$$(9) \quad (\mathfrak{V}\psi)(x) = \int_\Gamma G(x-y) \psi(y) d\Gamma(y),$$

$$(10) \quad (\mathfrak{K}v)(x) = \int_\Gamma \partial_{n(y)} G(x-y) v(y) d\Gamma(y),$$

$$(11) \quad (\mathfrak{W}v)(x) = -\partial_{n(x)} \int_\Gamma \partial_{n(y)} G(x-y) v(y) d\Gamma(y).$$

By continuous extension, these definitions provide linear boundary integral operators $\mathfrak{V} \in L(H^{-1/2}(\Gamma); H^{1/2}(\Gamma))$, $\mathfrak{K} \in L(H^{1/2}(\Gamma); H^{1/2}(\Gamma))$, and $\mathfrak{W} \in L(H^{1/2}(\Gamma); H^{-1/2}(\Gamma))$ as well as

$\mathfrak{K}' \in L(H^{-1/2}(\Gamma); H^{-1/2}(\Gamma))$. By scaling of Ω , we may assume that $\text{diam}(\Omega) < 1$ to ensure the uniform ellipticity of \mathfrak{B} , i.e.

$$\|\psi\|_{H^{-1/2}(\Gamma)}^2 \lesssim \langle \psi, \mathfrak{B}\psi \rangle_{\Gamma} \quad \text{for all } \psi \in H^{-1/2}(\Gamma).$$

The link between (5) and (7) is provided by $u = u^{\text{int}}$ and $\phi = \nabla u^{\text{ext}} \cdot n$, and u^{ext} is then given by the third Green's formula

$$(12) \quad u^{\text{ext}}(x) = \tilde{\mathfrak{K}}(u - u_0)(x) - \tilde{\mathfrak{B}}\phi(x) \quad \text{for } x \in \Omega^{\text{ext}},$$

where the potentials $\tilde{\mathfrak{B}}$ and $\tilde{\mathfrak{K}}$ formally denote the operators \mathfrak{B} and \mathfrak{K} , but are now evaluated in Ω^{ext} instead of Γ . Note carefully that we do not use a notational difference for the function $u \in H^1(\Omega)$ and its trace $u \in H^{1/2}(\Gamma)$, for which we compute the boundary integrals $\mathfrak{W}u$ and $(\mathfrak{K} - \frac{1}{2})u$ in (7).

It is well-known that (7) is well-posed in the sense that it allows for a unique solution $(u, \phi) \in \mathcal{H}$. Since we need some arguments from [11] below, we briefly recall the corresponding proof of [11, Corollary 2]: First, the second equation of (7) is equivalently written as

$$\phi = \mathfrak{B}^{-1}(\mathfrak{K} - \frac{1}{2})(u - u_0).$$

This identity may be used to eliminate ϕ in the first equation of (7). This gives rise to the exterior Dirichlet-to-Neumann map (or: exterior Steklov-Poincaré operator)

$$(13) \quad \mathfrak{S} := \mathfrak{W} + (\mathfrak{K}' - \frac{1}{2})\mathfrak{B}^{-1}(\mathfrak{K} - \frac{1}{2}) \in L(H^{1/2}(\Gamma); H^{-1/2}(\Gamma))$$

which is elliptic, i.e. $\langle \mathfrak{S}v, v \rangle \gtrsim \|v\|_{H^{1/2}(\Gamma)}^2$ for all $v \in H^{1/2}(\Gamma)$, see [11, Lemma 4] and Appendix A below. We define the (in general nonlinear) operator

$$(14) \quad \mathfrak{A} : H^1(\Omega) \rightarrow \tilde{H}^{-1}(\Omega) \quad \text{by} \quad \mathfrak{A}(u)[v] := \langle A\nabla u, \nabla v \rangle_{\Omega} + \langle \mathfrak{S}u, v \rangle_{\Gamma}$$

and the right-hand side

$$(15) \quad L \in \tilde{H}^{-1}(\Omega) \quad \text{by} \quad Lv := \langle f, v \rangle_{\Omega} + \langle \phi_0 + \mathfrak{S}u_0, v \rangle_{\Gamma}.$$

Then, (7) is equivalently recast into the operator equation

$$(16) \quad \mathfrak{A}(u) = L \quad \text{in } \tilde{H}^{-1}(\Omega).$$

The operator \mathfrak{A} is Lipschitz continuous and strongly monotone, i.e.

$$\|\mathfrak{A}u - \mathfrak{A}v\|_{\tilde{H}^{-1}(\Omega)} \lesssim \|u - v\|_{H^1(\Omega)} \quad \text{as well as} \quad \|u - v\|_{H^1(\Omega)}^2 \lesssim \langle \mathfrak{A}u - \mathfrak{A}v, u - v \rangle_{\Omega}.$$

Consequently, the main theorem on monotone operators proves that (16) and thus (7) have a unique solution.

2.2. Galerkin Discretization. Let \mathcal{T}_{ℓ} be a regular triangulation of Ω into triangles $T_j \in \mathcal{T}_{\ell}$ and \mathcal{E}_{ℓ} be a partition of the coupling boundary Γ into piecewise affine line segments $E_j \in \mathcal{E}_{\ell}$. Let $\text{diam}(\omega)$ denote the Euclidean diameter of a set $\omega \subset \mathbb{R}^2$. For $x \in \tau \in \mathcal{T}_{\ell} \cup \mathcal{E}_{\ell}$, we define the local mesh-width function by $h_{\ell}(x) := \text{diam}(\tau)$.

For the discretization, we use a conforming discretization with continuous and \mathcal{T}_{ℓ} -piecewise affine finite elements in Ω and \mathcal{E}_{ℓ} -piecewise constants on Γ , i.e. the discrete spaces read

$$(17) \quad \mathcal{X}_{\ell} := \mathcal{S}^1(\mathcal{T}_{\ell}) \times \mathcal{P}^0(\mathcal{E}_{\ell}) \quad \subset \quad H^1(\Omega) \times H^{-1/2}(\Gamma) = \mathcal{H}.$$

We stress that the analysis does not enforce any coupling of \mathcal{E}_ℓ and \mathcal{T}_ℓ . In particular, we do not need to assume that the boundary mesh \mathcal{E}_ℓ coincides with the restriction $\mathcal{T}_\ell|_\Gamma$. However, for the ease of implementation, we will consider $\mathcal{E}_\ell = \mathcal{T}_\ell|_\Gamma$ in the numerical experiments of Section 5.

The Galerkin formulation of (7) then reads as follows: Find $\mathbf{U}_\ell^* = (U_\ell^*, \Phi_\ell^*) \in \mathcal{X}_\ell$ such that

$$(18) \quad \begin{cases} \langle A\nabla U_\ell^*, \nabla V_\ell \rangle_\Omega + \langle \mathfrak{W}U_\ell^* + (\mathfrak{K}' - \frac{1}{2})\Phi_\ell^*, V_\ell \rangle_\Gamma = \langle f, V_\ell \rangle_\Omega + \langle \phi_0 + \mathfrak{W}u_0, V_\ell \rangle_\Gamma, \\ \langle \Psi_\ell, \mathfrak{B}\Phi_\ell^* - (\mathfrak{K} - \frac{1}{2})U_\ell^* \rangle_\Gamma = -\langle \Psi_\ell, (\mathfrak{K} - \frac{1}{2})u_0 \rangle_\Gamma, \end{cases}$$

for all $\mathbf{V}_\ell = (V_\ell, \Psi_\ell) \in \mathcal{X}_\ell$.

To proof the unique solvability of (18), the analysis of [11, Section 3] mimics the proof of the continuous case. Namely, (18) is equivalently rewritten in terms of a (in general nonlinear) operator equation

$$(19) \quad \mathfrak{A}_\ell(U_\ell) = L_\ell \quad \text{in } \mathcal{S}^1(\mathcal{T}_\ell)^*,$$

where the nonlinear operator \mathfrak{A}_ℓ reads

$$(20) \quad \mathfrak{A}_\ell : \mathcal{S}^1(\mathcal{T}_\ell) \rightarrow \mathcal{S}^1(\mathcal{T}_\ell)^*, \quad \mathfrak{A}_\ell(U_\ell)[V_\ell] := \langle A\nabla U_\ell, \nabla V_\ell \rangle_\Omega + \langle \mathfrak{S}_\ell U_\ell, V_\ell \rangle_\Gamma,$$

cf. [11, Corollary 3]. Here, \mathfrak{S}_ℓ denotes a discrete Dirichlet-to-Neumann map, which arises from the elimination of Φ_ℓ^* in the first equation of (18). It can be shown that \mathfrak{S}_ℓ is uniformly elliptic, where the constant depends only on Ω but not on \mathcal{X}_ℓ , see Appendix A. As in the continuous case, this implies that the Lipschitz continuous operator \mathfrak{A}_ℓ is strongly monotone. Again, the main theorem on monotone operators proves the unique solvability of (19) and thus of (18).

Moreover, uniform ellipticity of \mathfrak{S}_ℓ implies that the unique discrete solution $\mathbf{U}_\ell^* \in \mathcal{X}_\ell$ is quasi optimal in the sense of the Céa lemma

$$(21) \quad \|\mathbf{u} - \mathbf{U}_\ell^*\| \leq C_1 \min_{\mathbf{v}_\ell \in \mathcal{X}_\ell} \|\mathbf{u} - \mathbf{v}_\ell\|,$$

where the constant $C_1 > 0$ depends only on Ω , see [11, Corollary 3]. Here, the natural energy norm on the energy space \mathcal{H} is given by

$$(22) \quad \|\mathbf{v}\| = (\|v\|_{H^1(\Omega)}^2 + \langle \psi, \mathfrak{B}\psi \rangle_\Gamma)^{1/2} \quad \text{for } \mathbf{v} := (v, \psi) \in \mathcal{H}.$$

We stress that \mathcal{H} associated with $\|\cdot\|$ is a Hilbert space, since $\|\psi\|_{\mathfrak{B}} := \langle \psi, \mathfrak{B}\psi \rangle_\Gamma^{1/2}$ defines an equivalent norm on $H^{-1/2}(\Gamma)$.

2.3. Perturbed Galerkin Discretization. One drawback of the discrete formulation (18) is that the right-hand side involves the evaluation of $\mathfrak{W}u_0$ and $\mathfrak{K}u_0$, which can hardly be performed analytically. Moreover, so-called *fast methods for boundary integral operators* usually deal with discrete functions, cf. [26]. Therefore, we propose to approximate at least the given boundary data $u_0 \in H^{1/2}(\Gamma)$ by appropriate discrete functions and proceed analogously to [4]: To that end, we assume additional regularity $u_0 \in H^1(\Gamma)$. According to the Sobolev inequality in 1D, u_0 is continuous. Therefore, we may consider the nodal interpolant

$$(23) \quad U_{0,\ell} := I_\ell u_0 = \sum_{j=1}^n u_0(z_j) \zeta_j \in \mathcal{S}^1(\mathcal{E}_\ell),$$

where $z_j \in \Gamma$ denotes a node of \mathcal{E}_ℓ and where ζ_j is the associated \mathcal{E}_ℓ -piecewise linear and continuous hat function, i.e., $\zeta_j(z_k) = \delta_{jk}$. Now, the perturbed Galerkin formulation reads as follows: Find $\mathbf{U}_\ell = (U_\ell, \Phi_\ell) \in \mathcal{X}_\ell$ such that

$$(24) \quad \begin{cases} \langle A\nabla U_\ell, \nabla V_\ell \rangle_\Omega + \langle \mathfrak{W}U_\ell + (\mathfrak{K}' - \frac{1}{2})\Phi_\ell, V_\ell \rangle_\Gamma = \langle f, V_\ell \rangle_\Omega + \langle \phi_0 + \mathfrak{W}U_{0,\ell}, V_\ell \rangle_\Gamma, \\ \langle \Psi_\ell, \mathfrak{V}\Phi_\ell - (\mathfrak{K} - \frac{1}{2})U_\ell \rangle_\Gamma = -\langle \Psi_\ell, (\mathfrak{K} - \frac{1}{2})U_{0,\ell} \rangle_\Gamma, \end{cases}$$

for all $\mathbf{V}_\ell = (V_\ell, \Psi_\ell) \in \mathcal{X}_\ell$. Compared to (18), the only difference is that (24) involves the approximate data $U_{0,\ell}$ instead of u_0 on the right-hand side. Consequently, the same arguments as before prove that (24) has a unique solution.

3. A POSTERIORI ERROR ESTIMATION

3.1. Local Mesh-Refinement. For the local refinement of the volume mesh \mathcal{T}_ℓ , we use newest vertex bisection, where marked triangles $T \in \mathcal{T}_\ell$ are refined by $\text{bise}_3(T)$. We refer to [29, Chapter 5] for details on newest vertex bisection. The mesh $\widehat{\mathcal{T}}_\ell$ is obtained from uniform bise_3 -refinement of \mathcal{T}_ℓ . This ensures uniform shape regularity of the triangulations \mathcal{T}_ℓ and $\widehat{\mathcal{T}}_\ell$. More precisely, the shape regularity constant

$$(25) \quad \sigma(\mathcal{T}_\ell) := \max \{ \text{diam}(T)^2 / |T| : T \in \mathcal{T}_\ell \}$$

depends only on the initial mesh \mathcal{T}_0 , i.e.

$$(26) \quad \max \{ \sup_{\ell \in \mathbb{N}} \sigma(\mathcal{T}_\ell), \sup_{\ell \in \mathbb{N}} \sigma(\widehat{\mathcal{T}}_\ell) \} \leq C \sigma(\mathcal{T}_0),$$

where $C >$ depends only on the labelling of the reference edges in \mathcal{T}_0 . Furthermore, there holds nestedness of the associated spaces

$$\mathcal{S}^1(\mathcal{T}_\ell) \subset \mathcal{S}^1(\mathcal{T}_{\ell+1}) \subseteq \mathcal{S}^1(\widehat{\mathcal{T}}_\ell) \subset \mathcal{S}^1(\widehat{\mathcal{T}}_{\ell+1}).$$

For the local refinement of the boundary mesh \mathcal{E}_ℓ , we use bisection of the marked elements, i.e. marked elements $E \in \mathcal{E}_\ell$ are refined into two son elements with halved diameter. Since the error estimates below depend on the K -mesh constant (or: local mesh-ratio)

$$(27) \quad \kappa(\mathcal{E}_\ell) := \max \{ \text{diam}(E) / \text{diam}(E') : E, E' \in \mathcal{E}_\ell \text{ with } E \cap E' \neq \emptyset \},$$

one has to do some additional marking to ensure

$$(28) \quad \sup_{T \in \mathcal{T}_\ell} \kappa(\mathcal{E}_\ell) \leq 2 \kappa(\mathcal{E}_0),$$

cf. [4, Section 2.2] for details. The mesh $\widehat{\mathcal{E}}_\ell$ is obtained from uniform refinement of \mathcal{E}_ℓ , whence $\kappa(\mathcal{E}_\ell) = \kappa(\widehat{\mathcal{E}}_\ell)$.

Alternatively, one may consider the boundary partition $\mathcal{E}_\ell := \mathcal{T}_\ell|_\Gamma$ induced by the triangulation \mathcal{T}_ℓ of Ω . Then, marking of an element $E \in \mathcal{E}_\ell$ means marking of certain edges of some triangles $T \in \mathcal{T}_\ell$ for newest vertex bisection. We stress that this also guarantees that marked elements E are split into two son elements of half length. Moreover, due to uniform shape regularity (26) of \mathcal{T}_ℓ , there automatically holds

$$(29) \quad \sup_{T \in \mathcal{T}_\ell} \kappa(\mathcal{E}_\ell) \leq C \kappa(\mathcal{E}_0),$$

with some constant $C > 0$ which depends only on \mathcal{T}_0 .

In any case, there again holds nestedness

$$\mathcal{P}^0(\mathcal{T}_\ell) \subset \mathcal{P}^0(\mathcal{T}_{\ell+1}) \subseteq \mathcal{P}^0(\widehat{\mathcal{T}}_\ell) \subset \mathcal{P}^0(\widehat{\mathcal{T}}_{\ell+1}).$$

Finally, we consider the discrete spaces $\mathcal{X}_\ell := \mathcal{S}^1(\mathcal{T}_\ell) \times \mathcal{P}^0(\mathcal{E}_\ell)$ as well as $\widehat{\mathcal{X}}_\ell := \mathcal{S}^1(\widehat{\mathcal{T}}_\ell) \times \mathcal{P}^0(\widehat{\mathcal{E}}_\ell)$. We note that

$$\mathcal{X}_\ell \subset \mathcal{X}_{\ell+1} \subseteq \widehat{\mathcal{X}}_\ell \subset \widehat{\mathcal{X}}_{\ell+1} \subset \mathcal{H},$$

where only the inclusions $\mathcal{X}_\ell \subset \mathcal{X}_{\ell+1}$, $\mathcal{X}_\ell \subset \widehat{\mathcal{X}}_\ell$, and $\widehat{\mathcal{X}}_\ell \subset \widehat{\mathcal{X}}_{\ell+1}$ are mandatory for the analysis below.

3.2. A Posteriori Error Control for Data Approximation. Instead of solving the non-perturbed Galerkin formulation (18) of the weak formulation (7), we solve the perturbed Galerkin formulation (24) in practice. Put differently, $\mathbf{U}_\ell = (U_\ell, \Phi_\ell) \in \mathcal{X}_\ell$ is the Galerkin approximation of the unique solution $\mathbf{u}_\ell = (u_\ell, \phi_\ell) \in \mathcal{H}$ of the perturbed formulation

$$(30) \quad \begin{cases} \langle A\nabla u_\ell, \nabla v \rangle_\Omega + \langle \mathfrak{W}u_\ell + (\mathfrak{K}' - \frac{1}{2})\phi_\ell, v \rangle_\Gamma = \langle f, v \rangle_\Omega + \langle \phi_0 + \mathfrak{W}U_{0,\ell}, v \rangle_\Gamma, \\ \langle \psi, \mathfrak{V}\phi_\ell - (\mathfrak{K} - \frac{1}{2})u_\ell \rangle_\Gamma = -\langle \psi, (\mathfrak{K} - \frac{1}{2})U_{0,\ell} \rangle_\Gamma, \end{cases}$$

for all $\mathbf{v} = (v, \psi) \in \mathcal{H}$. In this section, we aim to verify a computable upper bound to control the approximation errors $\|\mathbf{u} - \mathbf{u}_\ell\|$ and $\|\mathbf{U}_\ell^* - \mathbf{U}_\ell\|$, stated in the following proposition.

Proposition 1. *There holds the approximation error estimate*

$$(31) \quad C_2^{-1} \|\mathbf{U}_\ell^* - \mathbf{U}_\ell\| \leq \|\mathbf{u} - \mathbf{u}_\ell\| \leq C_3 \text{osc}_\ell, \quad \text{where } \text{osc}_\ell := \|h_\ell^{1/2}(u_0 - U_{0,\ell})'\|_{L^2(\Gamma)}.$$

Here, $(\cdot)'$ denotes the arclength derivative along Γ . The constant $C_2 > 0$ depends only on Ω , whereas $C_3 > 0$ additionally depends on the K -mesh constant $\kappa(\mathcal{E}_0)$.

The proof of (31) is essentially based on the following stability result.

Lemma 2. *Let $\mathbf{u} = (u, \phi) \in \mathcal{H}$ be the exact solution of (7) for given data $(f, u_0, \phi_0) \in \mathcal{D} := \widetilde{H}^{-1}(\Omega) \times H^{1/2}(\Gamma) \times H^{-1/2}(\Gamma)$. Let $\widetilde{\mathbf{u}} = (\widetilde{u}, \widetilde{\phi}) \in \mathcal{H}$ be the exact solution of (7) for given data $(\widetilde{f}, \widetilde{u}_0, \widetilde{\phi}_0) \in \mathcal{D}$. Let $\mathbf{U}_\ell^*, \widetilde{\mathbf{U}}_\ell^* \in \mathcal{X}_\ell$ be the respective Galerkin solutions of (18). Then,*

$$(32) \quad C_2^{-1} \|\mathbf{U}_\ell^* - \widetilde{\mathbf{U}}_\ell^*\| \leq \|\mathbf{u} - \widetilde{\mathbf{u}}\| \leq C_4 (\|f - \widetilde{f}\|_{\widetilde{H}^{-1}(\Omega)} + \|u_0 - \widetilde{u}_0\|_{H^{1/2}(\Gamma)} + \|\phi_0 - \widetilde{\phi}_0\|_{H^{-1/2}(\Gamma)}),$$

where the constants $C_2, C_4 > 0$ depend only on Ω .

Proof. We proceed as above in Section 2.1 to rewrite the weak formulations (7) for \mathbf{u} and $\widetilde{\mathbf{u}}$. Note that the second equations of both formulations are equivalently written as

$$\phi = \mathfrak{V}^{-1}(\mathfrak{K} - \frac{1}{2})(u - u_0) \quad \text{as well as} \quad \widetilde{\phi} = \mathfrak{V}^{-1}(\mathfrak{K} - \frac{1}{2})(\widetilde{u} - \widetilde{u}_0).$$

With the operator \mathfrak{A} from (14) and the right-hand sides $L(\cdot) \in \widetilde{H}^{-1}(\Omega)$ defined by

$$L(f, u_0, \phi_0)[v] := \langle f, v \rangle_\Omega + \langle \phi_0 + \mathfrak{S}u_0, v \rangle_\Gamma,$$

the variational formulations (7) are equivalently recast into the operator equations

$$\mathfrak{A}(u) = L(f, u_0, \phi_0) \quad \text{resp.} \quad \mathfrak{A}(\widetilde{u}) = L(\widetilde{f}, \widetilde{u}_0, \widetilde{\phi}_0).$$

As mentioned above, \mathfrak{A} is Lipschitz continuous and strongly monotone, whence bijective. Moreover, the inverse of a strongly monotone operator is Lipschitz continuous since $\|u - v\|_{H^1(\Omega)} \lesssim \|\mathfrak{A}u - \mathfrak{A}v\|_{\tilde{H}^{-1}(\Omega)}$. This and the continuity of \mathfrak{S} imply

$$\begin{aligned} \|u - \tilde{u}\|_{H^1(\Omega)} &\lesssim \|L(f, u_0, \phi_0) - L(\tilde{f}, \tilde{u}_0, \tilde{\phi}_0)\|_{\tilde{H}^{-1}(\Omega)} \\ &\leq \|f - \tilde{f}\|_{\tilde{H}^{-1}(\Omega)} + \|\phi_0 - \tilde{\phi}_0\|_{H^{-1/2}(\Gamma)} + \|\mathfrak{S}(u_0 - \tilde{u}_0)\|_{H^{-1/2}(\Gamma)} \\ &\lesssim \|f - \tilde{f}\|_{\tilde{H}^{-1}(\Omega)} + \|\phi_0 - \tilde{\phi}_0\|_{H^{-1/2}(\Gamma)} + \|u_0 - \tilde{u}_0\|_{H^1(\Omega)}. \end{aligned}$$

Next, the mapping properties of the integral operators \mathfrak{W} and \mathfrak{K} yield

$$\begin{aligned} \|\phi - \tilde{\phi}\|_{H^{-1/2}(\Gamma)} &= \|\mathfrak{W}^{-1}(\mathfrak{K} - \tfrac{1}{2})((u - \tilde{u}) - (u_0 - \tilde{u}_0))\|_{H^{-1/2}(\Gamma)} \\ &\lesssim \|u - \tilde{u}\|_{H^1(\Omega)} + \|u_0 - \tilde{u}_0\|_{H^1(\Omega)}. \end{aligned}$$

Combining the latter two estimates and $\|u - \tilde{u}\|_{H^1(\Omega)} \lesssim \|u - \tilde{u}\|_{H^1(\Omega)}$, we obtain

$$\|\mathbf{u} - \tilde{\mathbf{u}}\| \lesssim \|f - \tilde{f}\|_{\tilde{H}^{-1}(\Omega)} + \|\phi_0 - \tilde{\phi}_0\|_{H^{-1/2}(\Gamma)} + \|u_0 - \tilde{u}_0\|_{H^1(\Omega)}.$$

This proves the upper estimate in (32).

To estimate $\|\mathbf{U}_\ell^* - \tilde{\mathbf{U}}_\ell^*\|$, we use the same type of arguments with the discrete operator \mathfrak{A}_ℓ . For instance, we rewrite (18) as

$$\begin{cases} \langle A\nabla U_\ell^*, \nabla V_\ell \rangle_\Omega + \langle \mathfrak{W}U_\ell^* + (\mathfrak{K}' - \tfrac{1}{2})\Phi_\ell^*, V_\ell \rangle_\Gamma &= \langle A\nabla u, \nabla V_\ell \rangle_\Omega + \langle \mathfrak{W}u + (\mathfrak{K}' - \tfrac{1}{2})\phi, V_\ell \rangle_\Gamma, \\ \langle \Psi_\ell, \mathfrak{W}\Phi_\ell^* - (\mathfrak{K} - \tfrac{1}{2})U_\ell^* \rangle_\Gamma &= \langle \Psi_\ell, \mathfrak{W}\phi - (\mathfrak{K} - \tfrac{1}{2})u \rangle_\Gamma, \end{cases}$$

for all $\mathbf{V}_\ell = (V_\ell, \Phi_\ell) \in \mathcal{X}_\ell$. With the discrete Steklov-Poincaré operator \mathfrak{S}_ℓ and the operator \mathfrak{A}_ℓ , this becomes

$$\mathfrak{A}_\ell U_\ell^* = L_\ell(u, \phi),$$

with a certain right-hand side $L_\ell(u, \phi) \in \mathcal{S}^1(\mathcal{T}_\ell)^*$. Replacing (u, ϕ) by $(\tilde{u}, \tilde{\phi})$, we obtain the discrete operator formulation for \tilde{U}_ℓ^* . It is easily seen that Lipschitz continuity of the inverse of \mathfrak{A}_ℓ thus yields

$$\|U_\ell^* - \tilde{U}_\ell^*\|_{H^1(\Omega)} \lesssim \|L_\ell(u, \phi) - L_\ell(\tilde{u}, \tilde{\phi})\|_{\mathcal{S}^1(\mathcal{T}_\ell)^*} \lesssim \|\mathbf{u} - \tilde{\mathbf{u}}\|.$$

Using the discrete simple-layer potential, one additionally obtains

$$\|\Phi_\ell^* - \tilde{\Phi}_\ell^*\|_{H^{-1/2}(\Gamma)} \lesssim \|U_\ell^* - \tilde{U}_\ell^*\|_{H^1(\Omega)} + \|\mathbf{u} - \tilde{\mathbf{u}}\| \lesssim \|\mathbf{u} - \tilde{\mathbf{u}}\|.$$

Altogether, we thus see $\|\mathbf{U}_\ell^* - \tilde{\mathbf{U}}_\ell^*\| \lesssim \|\mathbf{u} - \tilde{\mathbf{u}}\|$ and conclude the proof. \square

The a posteriori error control of the approximation of u_0 by $U_{0,\ell}$ is now done via an approximation result from [6, Theorem 1]. Our formulation in Equation (33), taken from [16, Lemma 2.2], is a consequence of the latter.

Lemma 3. *With $I_\ell : H^1(\Gamma) \rightarrow \mathcal{S}^1(\mathcal{E}_\ell)$ the nodal interpolation operator and $\Pi_\ell : L^2(\Gamma) \rightarrow \mathcal{P}^0(\mathcal{E}_\ell)$ the L^2 -orthogonal projection, there holds $\Pi_\ell(v') = (I_\ell v)'$, where $(\cdot)'$ denotes the arc-length derivative. Moreover, there holds the approximation result*

$$(33) \quad C_5^{-1} \|v - I_\ell v\|_{H^{1/2}(\Gamma)} \leq \|h_\ell^{1/2}(v - I_\ell v)'\|_{L^2(\Gamma)} \leq \|h_\ell^{1/2}v'\|_{L^2(\Gamma)} \quad \text{for all } v \in H^1(\Gamma),$$

and the constant $C_5 > 0$ depends only on Γ and $\kappa(\mathcal{E}_0)$. \square

Proof of Proposition 1. According to Lemma 2, there holds

$$\|\mathbf{U}_\ell^* - \mathbf{U}_\ell\| \lesssim \|\mathbf{u} - \mathbf{u}_\ell\| \lesssim \|u_0 - U_{0,\ell}\|_{H^{1/2}(\Gamma)}.$$

By choice of the discrete approximation $U_{0,\ell} = I_\ell u_0$, the approximation estimate (33) yields

$$\|u_0 - U_{0,\ell}\|_{H^{1/2}(\Gamma)} \lesssim \|h_\ell^{1/2}(u_0 - U_{0,\ell})'\|_{L^2(\Gamma)}.$$

This concludes the proof. \square

3.3. Saturation Assumption and $(h - h/2)$ -Error Estimator. Let $\widehat{\mathcal{T}}_\ell$ and $\widehat{\mathcal{E}}_\ell$ be the uniform refinements of \mathcal{T}_ℓ and \mathcal{E}_ℓ , respectively, and define

$$\widehat{\mathcal{X}}_\ell = \mathcal{S}^1(\widehat{\mathcal{T}}_\ell) \times \mathcal{P}^0(\widehat{\mathcal{E}}_\ell).$$

In this section, we consider the canonical $(h - h/2)$ -error estimators

$$(34) \quad \eta_\ell^* := \|\widehat{\mathbf{U}}_\ell^* - \mathbf{U}_\ell^*\| \quad \text{and} \quad \eta_\ell := \|\widehat{\mathbf{U}}_\ell - \mathbf{U}_\ell\|.$$

Here, $\widehat{\mathbf{U}}_\ell^*, \widehat{\mathbf{U}}_\ell \in \widehat{\mathcal{X}}_\ell$ are the Galerkin solutions of (18) and (24) with respect to the uniformly refined meshes. We remark that due to the non-locality of $\|\cdot\|_{\mathfrak{B}}$, the error estimator η_ℓ does not provide any information where to refine the boundary partition \mathcal{E}_ℓ . This will be different for the error estimators considered in the subsequent section.

Lemma 4. *There is a constant $C_6 > 0$ which depends only on Ω such that*

$$(35) \quad \eta_\ell^* \leq C_6 \|\mathbf{u} - \mathbf{U}_\ell^*\|.$$

Under the so-called saturation assumption

$$(36) \quad \|\mathbf{u} - \widehat{\mathbf{U}}_\ell^*\| \leq C_{\text{sat}} \|\mathbf{u} - \mathbf{U}_\ell^*\|$$

with some ℓ -independent constant $0 < C_{\text{sat}} < 1$, there holds

$$(37) \quad \|\mathbf{u} - \mathbf{U}_\ell^*\| \leq \frac{1}{1 - C_{\text{sat}}} \eta_\ell^*.$$

Proof. To prove (35), we use $\mathbf{U}_\ell^* \in \mathcal{X}_\ell \subset \widehat{\mathcal{X}}_\ell$ and the quasi-optimality (21). This and the triangle inequality yield

$$\eta_\ell^* \leq \|\mathbf{u} - \widehat{\mathbf{U}}_\ell^*\| + \|\mathbf{u} - \mathbf{U}_\ell^*\| \lesssim \|\mathbf{u} - \mathbf{U}_\ell^*\|.$$

For the converse inequality, the triangle inequality and the saturation assumption (36) provide

$$\|\mathbf{u} - \mathbf{U}_\ell^*\| \leq \|\mathbf{u} - \widehat{\mathbf{U}}_\ell^*\| + \eta_\ell^* \leq C_{\text{sat}} \|\mathbf{u} - \mathbf{U}_\ell^*\| + \eta_\ell^*.$$

Rearranging the terms, we conclude (37). \square

Lemma 5. *There is a constant $C_7 > 0$ which depends only on Ω and $\kappa(\mathcal{E}_0)$, such that*

$$(38) \quad \eta_\ell \leq \eta_\ell^* + C_7 \text{osc}_\ell \quad \text{as well as} \quad \eta_\ell^* \leq \eta_\ell + C_7 \text{osc}_\ell.$$

Proof. The triangle inequality and Proposition 1 prove

$$\eta_\ell \leq \eta_\ell^* + \|\widehat{\mathbf{U}}_\ell^* - \widehat{\mathbf{U}}_\ell\| + \|\mathbf{U}_\ell^* - \mathbf{U}_\ell\| \leq \eta_\ell^* + 2C_3 \text{osc}_\ell.$$

The converse inequality follows along the same lines. \square

Proposition 6. *There is a constant $C_8 > 0$ which depends only on Ω and $\kappa(\mathcal{E}_0)$ such that*

$$(39) \quad C_8^{-1} \eta_\ell \leq \|\mathbf{u} - \mathbf{U}_\ell\| + \text{osc}_\ell.$$

Under the saturation assumption (36), there is a constant $C_9 > 0$ such that

$$(40) \quad C_9^{-1} \|\mathbf{u} - \mathbf{U}_\ell\| \leq \eta_\ell + \text{osc}_\ell.$$

Besides Ω and $\kappa(\mathcal{E}_0)$, the constant $C_9 > 0$ depends only on $C_{\text{sat}} > 0$.

Proof. The proof is a consequence of Lemma 4 and Lemma 5. For instance, there holds

$$\eta_\ell \lesssim \eta_\ell^* + \text{osc}_\ell \lesssim \|\mathbf{u} - \mathbf{U}_\ell^*\| + \text{osc}_\ell \lesssim \|\mathbf{u} - \mathbf{U}_\ell\| + \|\mathbf{U}_\ell - \mathbf{U}_\ell^*\| + \text{osc}_\ell \lesssim \|\mathbf{u} - \mathbf{U}_\ell\| + \text{osc}_\ell.$$

This proves (39), and (40) follows along the same lines. \square

3.4. Further $(\mathbf{h} - \mathbf{h}/2)$ -Type Error Estimators. Let $\widehat{\mathbf{U}}_\ell = (\widehat{U}_\ell, \widehat{\Phi}_\ell) \in \widehat{\mathcal{X}}_\ell$ be the Galerkin solution of (24) with respect to $\widehat{\mathcal{X}}_\ell$. In addition to the error estimator η_ℓ from (34), we introduce two further error estimators. First,

$$(41) \quad \mu_\ell := \left(\|(1 - I_\ell^T) \widehat{U}_\ell\|_{H^1(\Omega)}^2 + \|h_\ell^{1/2} (1 - \Pi_\ell) \widehat{\Phi}_\ell\|_{L^2(\Gamma)}^2 \right)^{1/2},$$

where $I_\ell^T : C(\overline{\Omega}) \rightarrow \mathcal{S}^1(\mathcal{T}_\ell)$ denotes the nodal interpolation operator and where $\Pi_\ell : L^2(\Gamma) \rightarrow \mathcal{P}^0(\mathcal{E}_\ell)$ denotes the $L^2(\Gamma)$ -orthogonal projection. Second,

$$(42) \quad \tilde{\mu}_\ell := \left(\|(1 - \Pi_\ell^{(1)}) \widehat{U}_\ell\|_{L^2(\Omega)}^2 + \|(1 - \Pi_\ell^{(0)}) \nabla \widehat{U}_\ell\|_{L^2(\Omega)}^2 + \|h_\ell^{1/2} (1 - \Pi_\ell) \widehat{\Phi}_\ell\|_{L^2(\Gamma)}^2 \right)^{1/2},$$

where $\Pi_\ell^{(p)} : L^2(\Omega) \rightarrow \mathcal{P}^p(\mathcal{T}_\ell)$ denote the $L^2(\Omega)$ -orthogonal projections.

The local contributions of μ_ℓ and $\tilde{\mu}_\ell$ are denoted by

$$(43) \quad \begin{aligned} \mu_\ell(T)^2 &= \|(1 - I_\ell^T) \widehat{U}_\ell\|_{H^1(T)}^2 \\ \tilde{\mu}_\ell(T)^2 &= \|(1 - \Pi_\ell^{(1)}) \widehat{U}_\ell\|_{L^2(T)}^2 + \|(1 - \Pi_\ell^{(0)}) \nabla \widehat{U}_\ell\|_{L^2(T)}^2 \end{aligned}$$

for triangles $T \in \mathcal{T}_\ell$ and by

$$(44) \quad \mu_\ell(E)^2 = \tilde{\mu}_\ell(E)^2 = \text{diam}(E) \|(1 - \Pi_\ell) \widehat{\Phi}_\ell\|_{L^2(E)}^2$$

for line segments $E \in \mathcal{E}_\ell$. Note that this definition results in

$$(45) \quad \mu_\ell^2 = \sum_{T \in \mathcal{T}_\ell} \mu_\ell(T)^2 + \sum_{E \in \mathcal{E}_\ell} \mu_\ell(E)^2 \quad \text{and} \quad \tilde{\mu}_\ell^2 = \sum_{T \in \mathcal{T}_\ell} \tilde{\mu}_\ell(T)^2 + \sum_{E \in \mathcal{E}_\ell} \tilde{\mu}_\ell(E)^2.$$

The following lemma provides certain equivalences of the introduced error estimators.

Lemma 7. *There are constants $C_{10}, C_{11}, C_{12} > 0$ such that*

$$(46) \quad C_{10}^{-1} \mu_\ell(T) \leq \tilde{\mu}_\ell(T) \leq \mu_\ell(T) \quad \text{for all } T \in \mathcal{T}_\ell$$

as well as

$$(47) \quad C_{12}^{-1} \tilde{\mu}_\ell \leq \eta_\ell \leq C_{11} \mu_\ell \quad \text{and} \quad \mu_\ell \leq C_{10} \tilde{\mu}_\ell.$$

The constant $C_{10} \geq 1$ depends only on the shape regularity constant $\sigma(\mathcal{T}_0)$. The constant $C_{11} > 0$ depends only on Ω , whereas $C_{12} > 0$ additionally depends on $\kappa(\mathcal{E}_0)$.

Proof. Since the orthogonal projections $\Pi_\ell^{(p)}$ are \mathcal{T}_ℓ -elementwise best approximation operators, the estimate $\tilde{\mu}_\ell(T) \leq \mu_\ell(T)$ is obvious. The converse inequality follows from a scaling argument. In particular, there holds $C_{10} \geq 1$. In view of (43)–(45), this also implies $\mu_\ell \leq C_{10}\tilde{\mu}_\ell$.

Moreover, the local best approximation properties of $\Pi_\ell^{(p)}$ also proves

$$\tilde{\mu}_\ell(T)^2 \leq \|\widehat{U}_\ell - U_\ell\|_{H^1(T)}^2 \quad \text{for all } T \in \mathcal{T}_\ell.$$

Using the \mathcal{E}_ℓ -elementwise best approximation property of Π_ℓ and the local inverse estimate from [19, Theorem 3.6], we obtain

$$\|h_\ell^{1/2}(1 - \Pi_\ell)\widehat{\Phi}_\ell\|_{L^2(\Gamma)} \leq \|h_\ell^{1/2}(\widehat{\Phi}_\ell - \Phi_\ell)\|_{L^2(\Gamma)} \lesssim \|\widehat{\Phi}_\ell - \Phi_\ell\|_{\mathfrak{B}},$$

where the constant depends only on Γ and an upper bound of $\kappa(\mathcal{E}_\ell)$. The combination of the last two inequalities proves $\tilde{\mu}_\ell \lesssim \eta_\ell$.

Finally, we aim at proving $\eta_\ell \lesssim \mu_\ell$. To that end, recall that \widehat{U}_ℓ solves (18) with \mathcal{X}_ℓ replaced by $\widehat{\mathcal{X}}_\ell$. This allows to rewrite (18) in the form

$$\begin{cases} \langle A\nabla U_\ell, \nabla V_\ell \rangle_\Omega + \langle \mathfrak{W}U_\ell + (\mathfrak{K}' - \frac{1}{2})\Phi_\ell, V_\ell \rangle_\Gamma &= \langle A\nabla \widehat{U}_\ell, \nabla V_\ell \rangle_\Omega + \langle \mathfrak{W}\widehat{U}_\ell + (\mathfrak{K}' - \frac{1}{2})\widehat{\Phi}_\ell, V_\ell \rangle_\Gamma, \\ \langle \Psi_\ell, \mathfrak{W}\Phi_\ell - (\mathfrak{K} - \frac{1}{2})U_\ell \rangle_\Gamma &= \langle \Psi_\ell, \mathfrak{W}\widehat{\Phi}_\ell - (\mathfrak{K} - \frac{1}{2})\widehat{U}_\ell \rangle_\Gamma \end{cases}$$

for all $\mathbf{V}_\ell = (V_\ell, \Psi_\ell) \in \mathcal{X}_\ell$. Replacing $\mathbf{V}_\ell \in \mathcal{X}_\ell$ in this formulation by a general test function $\mathbf{v} \in \mathcal{H}$, we obtain a new variational formulation. By definition, \widehat{U}_ℓ is the corresponding continuous solution. Put differently, \mathbf{U}_ℓ is even a Galerkin approximation of \widehat{U}_ℓ . Consequently, quasi-optimality (21) of the Galerkin scheme proves

$$\eta_\ell^2 = \|\widehat{U}_\ell - \mathbf{U}_\ell\|^2 \lesssim \min_{\mathbf{V}_\ell \in \mathcal{X}_\ell} \|\widehat{U}_\ell - \mathbf{V}_\ell\|^2 \leq \|(1 - I_\ell^T)\widehat{U}_\ell\|_{H^1(\Omega)}^2 + \|(1 - \Pi_\ell)\widehat{\Phi}_\ell\|_{\mathfrak{B}}^2.$$

Finally, it is an approximation result from [7, Theorem 4.1, Lemma 4.3] that

$$\|(1 - \Pi_\ell)\widehat{\Phi}_\ell\|_{\mathfrak{B}} \lesssim \|h_\ell^{1/2}(1 - \Pi_\ell)\widehat{\Phi}_\ell\|_{L^2(\Gamma)},$$

where the constant depends only on Γ , see also [15, Lemma 2.1]. The combination of the last two estimates thus yields $\eta_\ell \lesssim \mu_\ell$ and concludes the proof. \square

Theorem 8. *There is a constant $C_{13} > 0$ which depends only on Ω , $\kappa(\mathcal{E}_0)$, and $\sigma(\mathcal{T}_0)$ such that*

$$(48) \quad C_{13}^{-1} \mu_\ell \leq \|\mathbf{u} - \mathbf{U}_\ell\| + \text{osc}_\ell.$$

Under the saturation assumption (36), there is a constant $C_{14} > 0$ such that

$$(49) \quad C_{14}^{-1} \|\mathbf{u} - \mathbf{U}_\ell\| \leq \mu_\ell + \text{osc}_\ell.$$

Besides Ω and $\kappa(\mathcal{E}_0)$, the constant $C_9 > 0$ depends only on $C_{\text{sat}} > 0$. The same estimates hold for $\tilde{\mu}_\ell$ replacing μ_ℓ .

Proof. The proof is an obvious consequence of Proposition 6 and the equivalence of the introduced error estimators stated in Lemma 7. \square

4. CONVERGENT ADAPTIVE COUPLING

4.1. A Priori Convergence of Adaptive Algorithms. Before we state the adaptive algorithm and prove convergence of which, we claim the *a priori convergence* of adaptive mesh-refining algorithms. By this, we mean that the sequences \mathbf{U}_ℓ^* and \mathbf{U}_ℓ of discrete solutions always tend to certain limits \mathbf{u}_∞^* and \mathbf{u}_∞ , independently of how the mesh is actually refined. Note carefully, however, that we do not claim that \mathbf{u} coincides with one of the a priori limits \mathbf{u}_∞^* or \mathbf{u}_∞ .

To deal with the data approximation, we need the following convergence result, which will be applied for the approximate data $U'_{0,\ell} = (I_\ell u_0)' = \Pi_\ell(u'_0) \in H := L^2(\Gamma)$. A proof can be found in [3, 10, 23].

Lemma 9. *Suppose that H is a Hilbert space and $X_\ell \subseteq X_{\ell+1}$ is a sequence of closed subspaces of H . Let $\mathbb{P}_\ell : H \rightarrow X_\ell$ denote the orthogonal projection onto X_ℓ . Then, for any $x \in H$ and $x_\ell := \mathbb{P}_\ell x$, the limit $x_\infty := \lim_{\ell \rightarrow \infty} x_\ell \in H$ exists. \square*

Proposition 10. *Let \mathcal{T}_ℓ and \mathcal{E}_ℓ be a sequence of meshes with corresponding nested spaces*

$$\mathcal{X}_\ell \subset \mathcal{X}_{\ell+1}.$$

Let $\mathbf{U}_\ell^ \in \mathcal{X}_\ell$ and $\mathbf{U}_\ell \in \mathcal{X}_\ell$ be the corresponding Galerkin solutions of (18) and (24), respectively. Then, there are limits $\mathbf{u}_\infty^*, \mathbf{u}_\infty \in \mathcal{H}$ such that*

$$(15) \quad \lim_{\ell \rightarrow \infty} \|\mathbf{u}_\infty^* - \mathbf{U}_\ell^*\| = 0 = \lim_{\ell \rightarrow \infty} \|\mathbf{u}_\infty - \mathbf{U}_\ell\|$$

Proof of a priori convergence of \mathbf{U}_ℓ^ .* We define the space \mathcal{X}_∞ as the closure of $\bigcup_{\ell=0}^\infty \mathcal{X}_\ell$. Then, \mathcal{X}_∞ is a closed subspace of \mathcal{H} which thus admits a unique Galerkin solution $\mathbf{u}_\infty^* \in \mathcal{X}_\infty$ of (18), see Appendix A. Arguing as in the proof of Lemma 7, we see that $\mathbf{U}_\ell^* \in \mathcal{X}_\ell$ is also a Galerkin solution of \mathbf{u}_∞^* and that there holds the Céa lemma

$$\|\mathbf{u}_\infty^* - \mathbf{U}_\ell^*\| \lesssim \min_{\mathbf{V}_\ell \in \mathcal{X}_\ell} \|\mathbf{u}_\infty^* - \mathbf{V}_\ell\|.$$

Let $\varepsilon > 0$. By definition of \mathcal{X}_∞ , we find some index $\ell_0 \in \mathbb{N}$ and some function $\mathbf{V}_{\ell_0} \in \mathcal{X}_{\ell_0}$ such that $\|\mathbf{u}_\infty^* - \mathbf{V}_{\ell_0}\| \leq \varepsilon$. From nestedness of \mathcal{X}_ℓ , we infer

$$\|\mathbf{u}_\infty^* - \mathbf{U}_\ell^*\| \lesssim \|\mathbf{u}_\infty^* - \mathbf{V}_{\ell_0}\| \leq \varepsilon$$

for all $\ell \geq \ell_0$. This proves convergence $\lim_{\ell \rightarrow \infty} \mathbf{U}_\ell^* = \mathbf{u}_\infty^*$. \square

Proof of a priori convergence of \mathbf{U}_ℓ . In 1D, the nodal interpolation operator $I_\ell : H^1(\Gamma) \rightarrow \mathcal{S}^1(\mathcal{E}_\ell)$ and the L^2 -orthogonal projection $\Pi_\ell : L^2(\Gamma) \rightarrow \mathcal{P}^0(\mathcal{E}_\ell)$ are linked through the well-known identity $(I_\ell v)' = \Pi_\ell(v')$. From nestedness $\mathcal{P}^0(\mathcal{E}_\ell) \subseteq \mathcal{P}^0(\mathcal{E}_{\ell+1})$, one may thus derive that the L^2 -limit

$$g = \lim_{\ell \rightarrow \infty} U'_{0,\ell} = \lim_{\ell \rightarrow \infty} \Pi_\ell(u'_0) \in L^2(\Gamma)$$

exists, see Lemma 9. In particular, the sequence $(U'_{0,\ell})_{\ell \in \mathbb{N}}$ of derivatives is a Cauchy sequence in $L^2(\Gamma)$. Let $\ell \geq k$. With the help of Lemma 3, we see

$$\begin{aligned} \|U_{0,\ell} - U_{0,k}\|_{H^{1/2}(\Gamma)} &= \|(1 - I_k)U_{0,\ell}\|_{H^{1/2}(\Gamma)} \lesssim \|h_\ell^{1/2}[(1 - I_k)U_{0,\ell}']\|_{L^2(\Gamma)} \\ &= \|h_\ell^{1/2}(U'_{0,\ell} - U'_{0,k})\|_{L^2(\Gamma)} \\ &\lesssim \|U'_{0,\ell} - U'_{0,k}\|_{L^2(\Gamma)} \xrightarrow{k,\ell \rightarrow \infty} 0. \end{aligned}$$

Consequently, the sequence $(U_{0,\ell})_{\ell \in \mathbb{N}}$ is a Cauchy sequence in $H^{1/2}(\Gamma)$ and thus convergent to some $H^{1/2}$ -limit

$$u_{0,\infty} = \lim_{\ell \rightarrow \infty} U_{0,\ell} \in H^{1/2}(\Gamma).$$

We now consider an auxiliary problem, where we only replace u_0 in the variational formulation (7) and its Galerkin discretization (18) by the obtained limit $u_{0,\infty}$. This provides a sequence $\mathbf{U}_{\infty,\ell}^* \in \mathcal{X}_\ell$ of Galerkin solutions. The already proven a priori convergence of \mathbf{U}_ℓ^* applies to this auxiliary problem as well. Consequently, the \mathcal{H} -limit

$$\mathbf{u}_\infty = \lim_{\ell \rightarrow \infty} \mathbf{U}_{\infty,\ell}^* \in \mathcal{H}$$

exists. The triangle inequality proves

$$\|\mathbf{u}_\infty - \mathbf{U}_\ell\| \leq \|\mathbf{u}_\infty - \mathbf{U}_{\infty,\ell}^*\| + \|\mathbf{U}_{\infty,\ell}^* - \mathbf{U}_\ell\|.$$

The first summand is known to tend to zero by definition of \mathbf{u}_∞ . For the second summand, we apply Lemma 2 to see

$$\|\mathbf{U}_{\infty,\ell}^* - \mathbf{U}_\ell\| \lesssim \|u_{0,\infty} - U_{0,\ell}\|_{H^{1/2}(\Gamma)} \xrightarrow{\ell \rightarrow \infty} 0$$

by definition of $u_{0,\infty}$. This concludes the proof. \square

4.2. Marking Criterion & Estimator Reduction. The marking is based on the Dörfler marking introduced in [14]. In view of Theorem 8, we consider the following refinement indicator

$$(51) \quad \varrho_\ell(\tau)^2 := \begin{cases} \mu_\ell(T)^2 & \text{for } \tau = T \in \mathcal{T}_\ell, \\ \mu_\ell(E)^2 + \text{osc}_\ell(E)^2 & \text{for } \tau = E \in \mathcal{E}_\ell, \end{cases}$$

where the local data oscillations read

$$(52) \quad \text{osc}_\ell(E) = \text{diam}(E) \|(u_0 - U_{\ell,0})'\|_{L^2(E)}^2 \quad \text{for } E \in \mathcal{E}_\ell.$$

By definition, there holds

$$(53) \quad \varrho_\ell^2 := \mu_\ell^2 + \text{osc}_\ell^2 = \sum_{\tau \in \mathcal{T}_\ell \cup \mathcal{E}_\ell} \varrho_\ell(\tau)^2.$$

For an arbitrary but fixed parameter $\theta \in (0, 1)$, we then determine a set $\mathcal{M}_\ell \subseteq \mathcal{T}_\ell \cup \mathcal{E}_\ell$ of marked elements with

$$(54) \quad \theta \varrho_\ell^2 \leq \sum_{\tau \in \mathcal{M}_\ell} \varrho_\ell(\tau)^2.$$

Based on the Dörfler marking (54) and the mesh-refinement rule, we next prove the crucial estimator reduction which is, however, not stated for ϱ_ℓ but for $\tilde{\varrho}_\ell$.

Lemma 11. *There are constants $\kappa \in (0, 1)$ and $C_{15} > 0$ such that*

$$(55) \quad \tilde{\varrho}_{\ell+1}^2 \leq \kappa \tilde{\varrho}_\ell^2 + C_{15} \|\widehat{\mathbf{U}}_{\ell+1} - \widehat{\mathbf{U}}_\ell\|^2,$$

where $\tilde{\varrho}_\ell^2 := \tilde{\mu}_\ell^2 + \text{osc}_\ell^2$. The contraction constant $\kappa \in (0, 1)$ depends only on the adaptivity parameter $\theta \in (0, 1)$, whereas the constant $C_{15} > 0$ additionally depends on Ω and $\kappa(\mathcal{E}_0)$.

Proof. Recall the identity $U'_{0,\ell} = (I_\ell u_0)' = \Pi_\ell(u'_0)$. First, for arbitrary $\delta > 0$, the Young inequality proves

$$\begin{aligned} \tilde{\varrho}_{\ell+1}^2 &= \|(1 - \Pi_{\ell+1}^{(1)})\widehat{U}_{\ell+1}\|_{L^2(\Omega)}^2 + \|(1 - \Pi_{\ell+1}^{(0)})\nabla\widehat{U}_{\ell+1}\|_{L^2(\Omega)}^2 + \|h_{\ell+1}^{1/2}(1 - \Pi_{\ell+1})\widehat{\Phi}_{\ell+1}\|_{L^2(\Gamma)}^2 \\ &\quad + \|h_{\ell+1}^{1/2}(1 - \Pi_{\ell+1})u'_0\|_{L^2(\Gamma)}^2 \\ &\leq (1 + \delta)\left(\|(1 - \Pi_{\ell+1}^{(1)})\widehat{U}_\ell\|_{L^2(\Omega)}^2 + \|(1 - \Pi_{\ell+1}^{(0)})\nabla\widehat{U}_\ell\|_{L^2(\Omega)}^2 + \|h_{\ell+1}^{1/2}(1 - \Pi_{\ell+1})\widehat{\Phi}_\ell\|_{L^2(\Gamma)}^2\right) \\ &\quad + (1 + \delta^{-1})\left(\|\widehat{U}_{\ell+1} - \widehat{U}_\ell\|_{L^2(\Omega)}^2 + \|\nabla\widehat{U}_{\ell+1} - \nabla\widehat{U}_\ell\|_{L^2(\Omega)}^2 + \|h_{\ell+1}^{1/2}(\widehat{\Phi}_{\ell+1} - \widehat{\Phi}_\ell)\|_{L^2(\Gamma)}^2\right) \\ &\quad + \|h_{\ell+1}^{1/2}(1 - \Pi_{\ell+1})u'_0\|_{L^2(\Gamma)}^2, \end{aligned}$$

where we have additionally used that all of the involved L^2 -orthogonal projections are even elementwise best approximation operators. Second, for $T \in \mathcal{T}_\ell \cap \mathcal{M}_\ell$ holds

$$\|(1 - \Pi_{\ell+1}^{(1)})\widehat{U}_\ell\|_{L^2(T)}^2 + \|(1 - \Pi_{\ell+1}^{(0)})\nabla\widehat{U}_\ell\|_{L^2(T)}^2 = 0,$$

whereas for $T \in \mathcal{T}_\ell \setminus \mathcal{M}_\ell$ holds

$$\|(1 - \Pi_{\ell+1}^{(1)})\widehat{U}_\ell\|_{L^2(T)}^2 + \|(1 - \Pi_{\ell+1}^{(0)})\nabla\widehat{U}_\ell\|_{L^2(T)}^2 \leq \tilde{\mu}_\ell(T)^2.$$

Note that \leq in the last estimate stems from the fact that an element $T \in \mathcal{T}_\ell \setminus \mathcal{M}_\ell$ may be refined to avoid hanging nodes, cf. Section 3.1. For $E \in \mathcal{E}_\ell \cap \mathcal{M}_\ell$ holds

$$\begin{aligned} \|h_{\ell+1}^{1/2}(1 - \Pi_{\ell+1})\widehat{\Phi}_\ell\|_{L^2(E)}^2 + \|h_{\ell+1}^{1/2}(1 - \Pi_{\ell+1})u'_0\|_{L^2(E)}^2 &= \frac{1}{2} \|h_\ell^{1/2}(1 - \Pi_{\ell+1})u'_0\|_{L^2(E)}^2 \\ &\leq \frac{1}{2} (\tilde{\mu}_\ell(E)^2 + \text{osc}_\ell(E)^2), \end{aligned}$$

whereas for $E \in \mathcal{E}_\ell \setminus \mathcal{M}_\ell$ holds

$$\|h_{\ell+1}^{1/2}(1 - \Pi_{\ell+1})\widehat{\Phi}_\ell\|_{L^2(E)}^2 + \|h_{\ell+1}^{1/2}(1 - \Pi_{\ell+1})u'_0\|_{L^2(E)}^2 \leq \tilde{\mu}_\ell(E)^2 + \text{osc}_\ell(E)^2.$$

Third, the local estimates are used to obtain

$$\begin{aligned}
& \|(1 - \Pi_{\ell+1}^{(1)})\widehat{U}_\ell\|_{L^2(\Omega)}^2 + \|(1 - \Pi_{\ell+1}^{(0)})\nabla\widehat{U}_\ell\|_{L^2(\Omega)}^2 + \|h_{\ell+1}^{1/2}(1 - \Pi_{\ell+1})\widehat{\Phi}_\ell\|_{L^2(\Gamma)}^2 \\
& \quad + \|h_{\ell+1}^{1/2}(1 - \Pi_{\ell+1})u'_0\|_{L^2(\Gamma)}^2 \\
& \leq \sum_{T \in \mathcal{T}_\ell \setminus \mathcal{M}_\ell} \tilde{\mu}_\ell(T)^2 + \frac{1}{2} \sum_{E \in \mathcal{E}_\ell \cap \mathcal{M}_\ell} (\tilde{\mu}_\ell(E)^2 + \text{osc}_\ell(E)^2) + \sum_{E \in \mathcal{E}_\ell \setminus \mathcal{M}_\ell} (\tilde{\mu}_\ell(E)^2 + \text{osc}_\ell(E)^2) \\
& \leq \sum_{T \in \mathcal{T}_\ell} \tilde{\mu}_\ell(T)^2 + \sum_{E \in \mathcal{E}_\ell} (\tilde{\mu}_\ell(E)^2 + \text{osc}_\ell(E)^2) \\
& \quad - \frac{1}{2} \left(\sum_{T \in \mathcal{T}_\ell \cap \mathcal{M}_\ell} \tilde{\mu}_\ell(T)^2 + \sum_{E \in \mathcal{E}_\ell \cap \mathcal{M}_\ell} (\tilde{\mu}_\ell(E)^2 + \text{osc}_\ell(E)^2) \right) \\
& = \tilde{\varrho}_\ell^2 - \frac{1}{2} \left(\sum_{T \in \mathcal{T}_\ell \cap \mathcal{M}_\ell} \tilde{\mu}_\ell(T)^2 + \sum_{E \in \mathcal{E}_\ell \cap \mathcal{M}_\ell} (\tilde{\mu}_\ell(E)^2 + \text{osc}_\ell(E)^2) \right).
\end{aligned}$$

Fourth, we employ the marking strategy (54) and the local equivalence (46) to see

$$\theta \tilde{\varrho}_\ell^2 \leq \theta \varrho_\ell^2 \leq \sum_{\tau \in \mathcal{M}_\ell} \varrho_\ell(\tau)^2 \leq C_{10} \sum_{T \in \mathcal{T}_\ell \cap \mathcal{M}_\ell} \tilde{\mu}_\ell(T)^2 + \sum_{E \in \mathcal{E}_\ell \cap \mathcal{M}_\ell} (\tilde{\mu}_\ell(E)^2 + \text{osc}_\ell(E)^2).$$

From $C_{10} \geq 1$, we thus infer

$$\tilde{\theta} \tilde{\varrho}_\ell^2 \leq \sum_{T \in \mathcal{T}_\ell \cap \mathcal{M}_\ell} \tilde{\mu}_\ell(T)^2 + \sum_{E \in \mathcal{E}_\ell \cap \mathcal{M}_\ell} (\tilde{\mu}_\ell(E)^2 + \text{osc}_\ell(E)^2)$$

with $\tilde{\theta} = \theta/C_{10} \in (0, 1)$. We now combine all foregoing estimates to see

$$\tilde{\varrho}_{\ell+1}^2 \leq (1 + \delta)(1 - \tilde{\theta}/2) \tilde{\varrho}_\ell^2 + (1 + \delta^{-1})(\|\widehat{U}_{\ell+1} - \widehat{U}_\ell\|_{H^1(\Omega)}^2 + \|h_{\ell+1}^{1/2}(\widehat{\Phi}_{\ell+1} - \widehat{\Phi}_\ell)\|_{L^2(\Gamma)}^2).$$

Since $(1 - \tilde{\theta}/2) < 1$, we may choose $\delta > 0$ with $\kappa := (1 + \delta)(1 - \tilde{\theta}/2) < 1$. Moreover, the local inverse estimate from [19, Theorem 3.6] proves

$$\|h_{\ell+1}^{1/2}(\widehat{\Phi}_{\ell+1} - \widehat{\Phi}_\ell)\|_{L^2(\Gamma)} \lesssim \|\widehat{\Phi}_{\ell+1} - \widehat{\Phi}_\ell\|_{\mathfrak{B}},$$

where the constant depends only on Γ and an upper bound of $\kappa(\mathcal{E}_\ell)$. Plugging this into the last estimate, we finally end up with (55). \square

4.3. Convergent Adaptive Algorithm. We now consider the following adaptive algorithm. We stress that an adaptive algorithm does neither know the a priori limit (u_∞, ϕ_∞) nor $(\widehat{u}_\infty, \widehat{\phi}_\infty)$.

Algorithm 12. INPUT: *Initial meshes* $(\mathcal{T}_0, \mathcal{E}_0)$ for $\ell := 0$, *adaptivity parameter* $\theta \in (0, 1)$.

- (i) *Generate uniformly refined meshes* $\widehat{\mathcal{T}}_\ell, \widehat{\mathcal{E}}_\ell$.
- (ii) *Compute discrete solution* $\widehat{U}_\ell \in \widehat{\mathcal{X}}_\ell$.
- (iii) *Compute refinement indicators* $\varrho_\ell(\tau)$ for all $\tau \in \mathcal{T}_\ell \cup \mathcal{E}_\ell$.
- (iv) *Determine set* $\mathcal{M}_\ell \subseteq \mathcal{T}_\ell \cup \mathcal{E}_\ell$ *which satisfies Dörfler marking* (54).
- (v) *Mark triangles* $T \in \mathcal{T}_\ell \cap \mathcal{M}_\ell$ *and boundary elements* $E \in \mathcal{E}_\ell \cap \mathcal{M}_\ell$ *for refinement.*
- (vi) *Generate new meshes* $(\mathcal{T}_{\ell+1}, \mathcal{E}_{\ell+1})$, *increase counter* $\ell \mapsto \ell + 1$, *and goto* (i).

OUTPUT: *Sequence of error estimators* $(\varrho_\ell)_{\ell \in \mathbb{N}}$ *and discrete solutions* $(\widehat{U}_\ell)_{\ell \in \mathbb{N}}$. \square

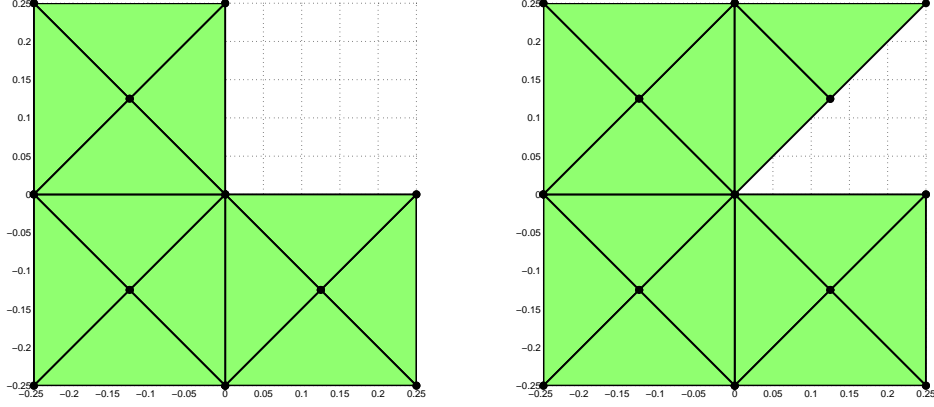


FIGURE 1. L-shaped (left) and Z-shaped domain (right) and initial triangulations \mathcal{T}_0 for the numerical experiments.

Theorem 13. *Algorithm 12 enforces*

$$(56) \quad \lim_{\ell \rightarrow \infty} \varrho_\ell = 0.$$

Under the saturation assumption (36), this implies convergence

$$(57) \quad \lim_{\ell \rightarrow \infty} \|(u, \phi) - (\hat{u}_\ell, \hat{\phi}_\ell)\| = 0 = \lim_{\ell \rightarrow \infty} \|(u, \phi) - (u_\ell, \phi_\ell)\|.$$

Proof. The idea of the proof goes back to [3]. We combine the estimator reduction (55) with the a priori convergence (50) and the estimator equivalence (47): First, we note that Lemma 11 provides an estimate of the type

$$\tilde{\varrho}_{\ell+1}^2 \leq \kappa \tilde{\varrho}_\ell^2 + \alpha_\ell$$

with some constant $\kappa \in (0, 1)$. According to Proposition 10 applied for $\hat{\mathcal{X}}_\ell$, the nonnegative sequence $\alpha_\ell \sim \|\hat{\mathbf{U}}_{\ell+1} - \hat{\mathbf{U}}_\ell\|^2$ tends to zero. It is a consequence of elementary calculus that this implies estimator convergence

$$\lim_{\ell \rightarrow \infty} \tilde{\varrho}_\ell = 0.$$

Now, the equivalence of $\tilde{\varrho}_\ell \sim \varrho_\ell$ —as a consequence of Lemma 7— concludes (56).

Under the saturation assumption (36), Proposition 6 states

$$\|\mathbf{u} - \mathbf{U}_\ell\| \lesssim \mu_\ell + \text{osc}_\ell \lesssim \varrho_\ell \xrightarrow{\ell \rightarrow \infty} 0$$

and thus convergence of \mathbf{U}_ℓ to \mathbf{u} . In this case, the quasi-optimality $\|\mathbf{u} - \hat{\mathbf{U}}_\ell\| \lesssim \|\mathbf{u} - \mathbf{U}_\ell\|$ also predicts convergence of $\hat{\mathbf{U}}_\ell$. \square

Remark. *It is a consequence of Theorem 13 that one obtains additional information on the a priori limits from the proof of Proposition 10. For instance, $\lim_\ell \text{osc}_\ell = 0$ predicts $u_{0,\infty} = u_0$, whence $\mathbf{u}_\infty^* = \mathbf{u}_\infty$ and $\hat{\mathbf{u}}_\infty^* = \hat{\mathbf{u}}_\infty$ if the latter denote the a priori limits of $\hat{\mathbf{U}}_\ell^*$ and $\hat{\mathbf{U}}_\ell$. Moreover, $\lim_\ell \mu_\ell = 0$ implies $\lim_\ell \eta_\ell = 0$ and thus even $\mathbf{u}_\infty = \hat{\mathbf{u}}_\infty$. \square*

5. NUMERICAL EXPERIMENTS

In this section, we present three numerical examples from [11] to demonstrate the advantages of the proposed adaptive FEM-BEM coupling and its superiority over uniform mesh-refinement. In all experiments, we prescribe the exact solution $(u^{\text{int}}, u^{\text{ext}})$ of the transmission problem (5), and the data (u_0, ϕ_0, f) are computed thereof. To simplify the implementation, we only consider the induced boundary partition $\mathcal{E}_\ell := \mathcal{T}_\ell|_\Gamma$.

Note that the contribution $\|\phi - \Phi_\ell\|_{\mathfrak{B}}$ to the error $\|\mathbf{u} - \mathbf{U}_\ell\|$ can hardly be computed analytically. However, according to Proposition 1 and the quasi optimality (21), there holds

$$\|\mathbf{u} - \mathbf{U}_\ell\| \lesssim \|\mathbf{u} - \mathbf{U}_\ell^*\| + \text{osc}_\ell \lesssim \|u - U_\ell\|_{H^1(\Omega)} + \min_{\Psi_\ell \in \mathcal{P}^0(\mathcal{E}_\ell)} \|\phi - \Psi_\ell\|_{\mathfrak{B}} + \text{osc}_\ell$$

with $\mathbf{u} = (u, \phi)$ and $\mathbf{U}_\ell = (U_\ell, \Phi_\ell)$. In all experiments, the exterior normal derivative has additional regularity $\phi \in L^2(\Gamma)$. We may therefore proceed as in the proof of Lemma 7 to obtain

$$\min_{\Psi_\ell \in \mathcal{P}^0(\mathcal{E}_\ell)} \|\phi - \Psi_\ell\|_{\mathfrak{B}} \leq \|(1 - \Pi_\ell)\phi\|_{\mathfrak{B}} \lesssim \|h_\ell^{1/2}(1 - \Pi_\ell)\phi\|_{L^2(\Gamma)} \leq \|h_\ell^{1/2}(\phi - \Phi_\ell)\|_{L^2(\Gamma)}$$

with $\Pi_\ell : L^2(\Gamma) \rightarrow \mathcal{P}^0(\mathcal{T}_\ell)$ being the L^2 -orthogonal projection. Altogether, we see that

$$(58) \quad \|\mathbf{u} - \mathbf{U}_\ell\| \lesssim \|u - U_\ell\|_{H^1(\Omega)} + \|h_\ell^{1/2}(\phi - \Phi_\ell)\|_{L^2(\Gamma)} + \text{osc}_\ell =: \text{err}_\ell(u) + \text{err}_\ell(\phi) + \text{osc}_\ell$$

provides a computable upper bound for the energy error. In the same spirit, the error estimator μ_ℓ is split into

$$(59) \quad \mu_\ell^2 = \sum_{T \in \mathcal{T}_\ell} \mu_\ell(T)^2 + \sum_{E \in \mathcal{E}_\ell} \mu_\ell(E)^2 =: \mu_\ell(u)^2 + \mu_\ell(\phi)^2.$$

Recall that Theorem 8 predicts

$$\mu_\ell(u) + \mu_\ell(\phi) + \text{osc}_\ell \lesssim \|\mathbf{u} - \mathbf{U}_\ell\| + \text{osc}_\ell \lesssim \mu_\ell(u) + \mu_\ell(\phi) + \text{osc}_\ell,$$

where the upper bound holds under the saturation assumption (36).

In the following, we plot the five quantities $\text{err}_\ell(u)$, $\text{err}_\ell(\phi)$, $\mu_\ell(u)$, $\mu_\ell(\phi)$, and osc_ℓ from (58)–(59) over the number $N = \#\mathcal{T}_\ell$ of triangles, where both axes are scaled logarithmically. We consider uniform mesh-refinement $\mathcal{T}_\ell = \mathcal{T}_\ell^{(\text{unif})}$ with $\mathcal{T}_\ell^{(\text{unif})} := \widehat{\mathcal{T}}_{\ell-1}$, cf. Section 3.1, as well as adaptive mesh-refinement, where the sequence of meshes $\mathcal{T}_\ell = \mathcal{T}_\ell^{(\text{adap})}$ is generated by Algorithm 12 with $\theta = 0.25$. Note that a decay with slope $-\alpha$ indicates some dependence $\mathcal{O}(N^{-\alpha})$. For uniform meshes with mesh-size h , this corresponds to $\mathcal{O}(h^{2\alpha})$. We stress that, by theory, an overall slope of $\alpha = 1/2$ is thus optimal with P1-finite elements.

For the adaptive mesh-refinement of Algorithm 12, recall that all integral operators have to be computed with respect to the fine mesh $\widehat{\mathcal{T}}_\ell$. Therefore, one usually takes the improved approximation $\widehat{U}_{0,\ell} \in \mathcal{S}^1(\widehat{\mathcal{T}}_\ell|_\Gamma)$ instead of $U_{0,\ell} \in \mathcal{S}^1(\mathcal{T}_\ell|_\Gamma)$. Consequently, we then consider $\widehat{\text{osc}}_\ell = \|h_\ell^{1/2}(u_0 - \widehat{U}_{0,\ell})'\|_{L^2(\Gamma)}$ instead of osc_ℓ . We stress that all results of this paper hold with osc_ℓ replaced by $\widehat{\text{osc}}_\ell$ as well. Moreover, although \mathbf{U}_ℓ is not needed by Algorithm 12, we nevertheless plot err_ℓ to give a fair comparison of uniform and adaptive mesh-refinement.

Besides the experimental convergence rates, we plot $\text{err}_\ell(u)$, $\text{err}_\ell(\phi)$, $\mu_\ell(u)$, $\mu_\ell(\phi)$, and osc_ℓ (resp. $\widehat{\text{osc}}_\ell$) over the computational time t_ℓ .

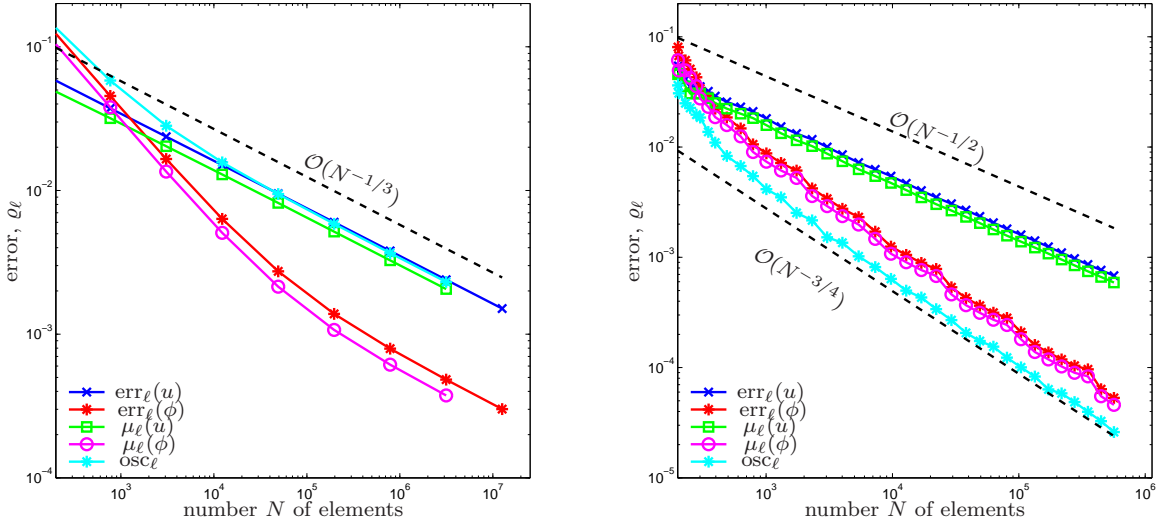


FIGURE 2. Estimators $\text{err}_\ell(u)$, $\text{err}_\ell(\phi)$, $\mu_\ell(u)$ and $\mu_\ell(\phi)$ from (58)–(59) as well as data oscillations osc_ℓ in linear Experiment 5.1, plotted over the number $N = \#\mathcal{T}_\ell$ of triangles for uniform (left) and adaptive mesh-refinement (right).

- For uniform mesh-refinement, $t_\ell = t_\ell^{(\text{unif})}$ is the time needed for ℓ uniform refinements of the initial mesh \mathcal{T}_0 to obtain \mathcal{T}_ℓ , plus the time for building and solving the Galerkin system with respect to \mathcal{X}_ℓ .

For adaptive mesh, refinement, the mesh \mathcal{T}_ℓ depends on the entire history of preceding meshes (and solutions). Therefore, the computational time has to be defined differently, where $t_{-1}^{(\text{adap})} := 0$.

- For adaptive mesh-refinement, $t_\ell = t_\ell^{(\text{adap})}$ is the sum of the time $t_{\ell-1}^{(\text{adap})}$ elapsed in prior steps of the adaptive algorithm, plus the time for generating the fine mesh $\widehat{\mathcal{T}}_\ell$, building and solving the Galerkin system with respect to $\widehat{\mathcal{X}}_\ell$, computing the local contributions of the data oscillations $\widehat{\text{osc}}_\ell$ and the error estimator μ_ℓ , element marking, and local refinement of \mathcal{T}_ℓ to generate $\mathcal{T}_{\ell+1}$.

Although this definition seems to favour uniform mesh-refinement, we think that it provides a fair comparison between uniform and adaptive mesh-refinement.

All experiments are conducted by use of MATLAB (Release 2009b) running on a common 64 Bit Linux system with 32 GB of RAM. Throughout, the occurring linear systems are solved by use of the MATLAB backslash operator. For the computation of the boundary integral operators, we use the MATLAB BEM library HILBERT, cf. [2]; see <http://www.asc.tuwien.ac.at/abem/hilbert>.

5.1. Linear Problem on L-Shaped Domain. We consider the L-shaped domain visualized in Figure 1. With $A : L^2(\Omega)^2 \rightarrow L^2(\Omega)^2$ being the identity, we prescribe the exact solution of (5) as

$$(60) \quad \begin{aligned} u^{\text{int}}(x, y) &= r^{2/3} \sin\left(\frac{2}{3}\varphi\right) && \text{in } \Omega^{\text{int}}, \\ u^{\text{ext}}(x, y) &= \log\left(\left(x + \frac{1}{8}\right)^2 + \left(y + \frac{1}{8}\right)^2\right)^{1/2} && \text{in } \Omega^{\text{ext}}, \end{aligned}$$

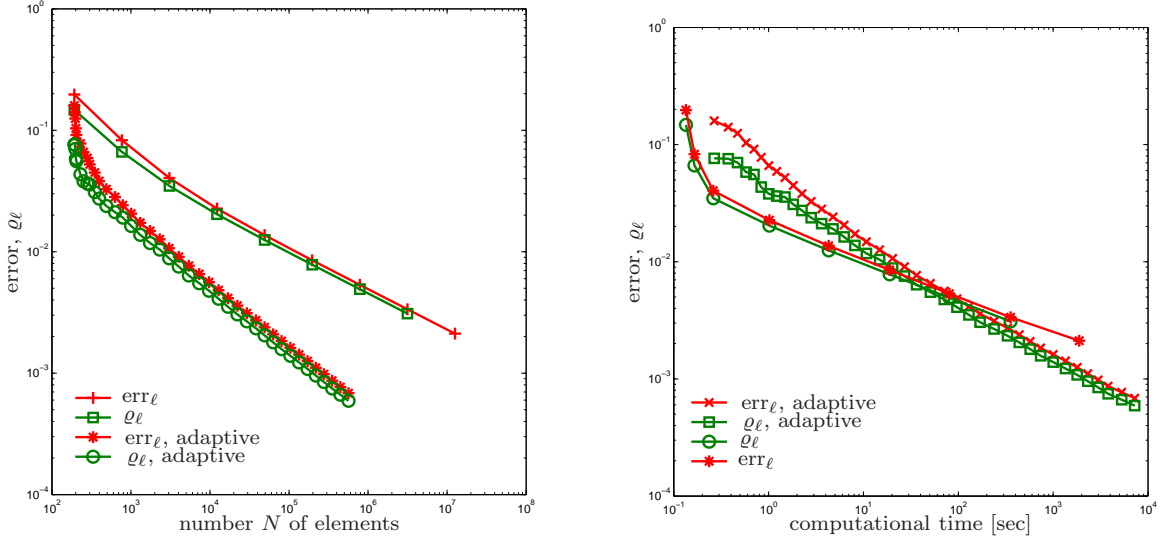


FIGURE 3. Comparison of uniform and adaptive mesh-refining in linear Experiment 5.1, where the error bound err_ℓ and the estimator ϱ_ℓ from (61) are plotted over the number $N = \#\mathcal{T}_\ell$ of triangles (left) and over the computational time (right).

where (r, φ) are the polar coordinates of $(x, y) \in \mathbb{R}^2$ with respect to $(0, 0)$. Clearly, the identity satisfies the assumptions of our model problem, and the FEM-BEM coupling (7) is linear. Recall that (u, ϕ) denotes the exact solution of (7) and note that $u = u^{\text{int}}$ has a generic singularity at the reentrant corner, whereas $\phi = \nabla u^{\text{ext}} \cdot n$ is piecewise smooth.

In Figure 2, we plot the convergence of the error quantities from (58)–(59). Since the interior solution has a generic singularity at the reentrant corner, uniform mesh-refinement leads to a suboptimal order of convergence $\alpha = 1/3$, i.e. we observe $\mathcal{O}(h^{2/3})$. For $\text{err}_\ell(u)$ and $\mu_\ell(u)$, this asymptotics is observed already on coarse meshes. For $\text{err}_\ell(\phi)$ and $\mu_\ell(\phi)$, a preasymptotic phase occurs. For adaptive mesh-refinement, we observe the optimal order of convergence $\alpha = 1/2$ for $\text{err}_\ell(u)$ and $\mu_\ell(u)$. Moreover, the terms $\text{err}_\ell(\phi)$ and $\mu_\ell(\phi)$ even converge with order $\alpha = 3/2$ which is optimal for the approximation of a smooth function by piecewise constants with respect to the $H^{-1/2}(\Gamma)$ -norm.

Figure 3 provides comparisons between uniform and adaptive mesh-refinement. We plot

$$(61) \quad \text{err}_\ell := (\text{err}_\ell(u)^2 + \text{err}_\ell(\phi)^2 + \text{osc}_\ell^2)^{1/2} \quad \text{and} \quad \varrho_\ell = (\mu_\ell(u)^2 + \mu_\ell(\phi)^2 + \text{osc}_\ell^2)^{1/2}$$

over the number $N = \#\mathcal{T}_\ell$ of elements as well as over the computational time. Both plots underline that the proposed adaptive algorithm is much superior to uniform mesh-refinement.

5.2. Nonlinear Problem on L-Shaped Domain. We consider the L-shaped domain visualized in Figure 1. We define

$$(62) \quad \rho(t) = 2 + \frac{1}{1+t} \quad \text{for } t > 0$$

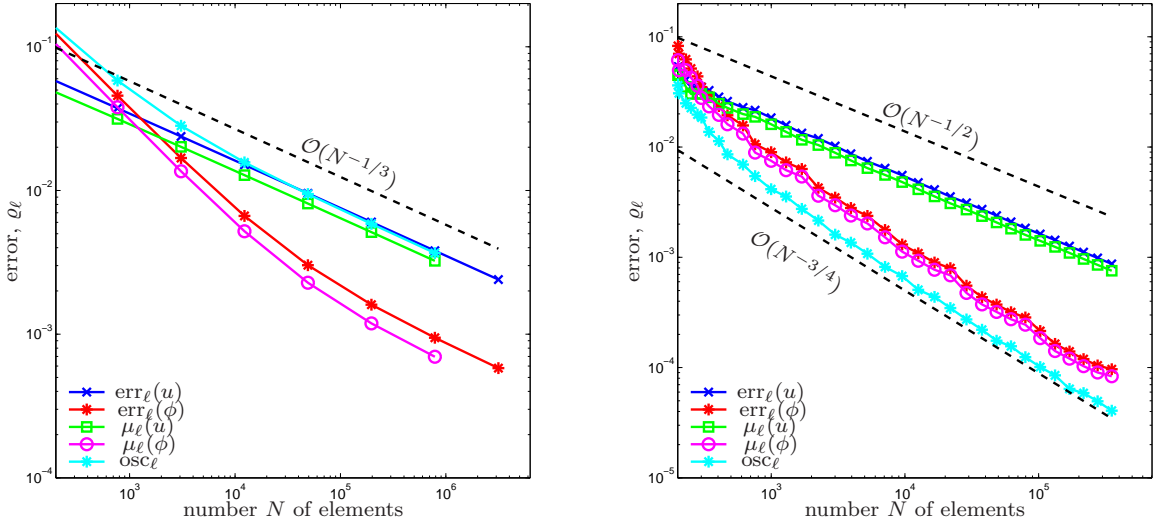


FIGURE 4. Estimators $\text{err}_\ell(u)$, $\text{err}_\ell(\phi)$, $\mu_\ell(u)$ and $\mu_\ell(\phi)$ from (58)–(59) as well as data oscillations osc_ℓ in nonlinear Experiment 5.2 on the L-shaped domain, plotted over the number $N = \#\mathcal{T}_\ell$ of triangles for uniform (left) and adaptive mesh-refinement (right).

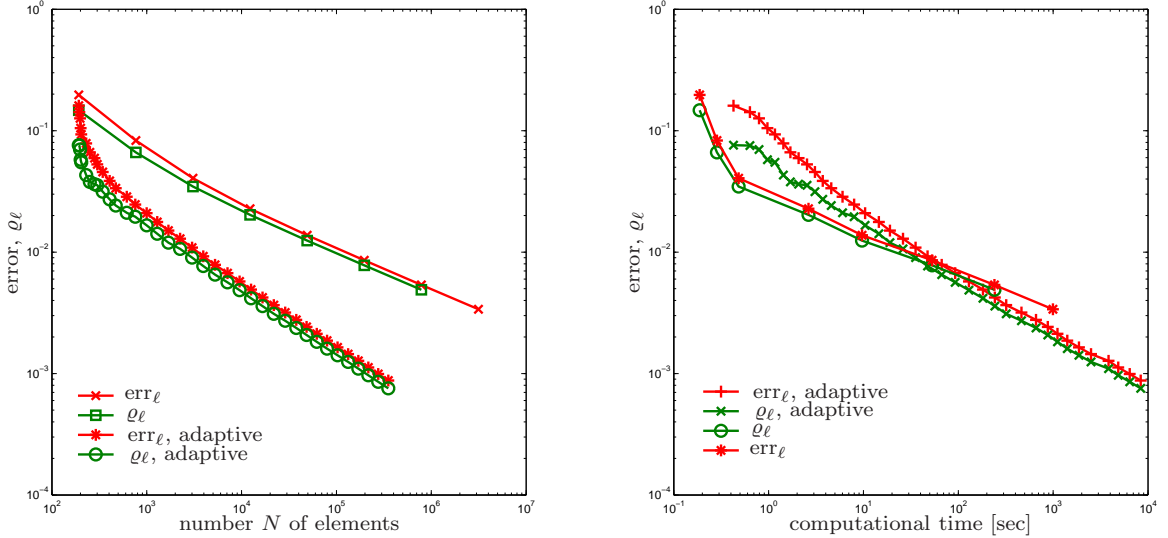


FIGURE 5. Comparison of uniform and adaptive mesh-refining in nonlinear Experiment 5.2 on the L-shaped domain, where the error bound err_ℓ and the estimator ϱ_ℓ from (61) are plotted over the number $N = \#\mathcal{T}_\ell$ of triangles (left) and over the computational time (right).

and note that the derivative satisfies $-1 \leq \rho'(t) < 0$. The nonlinear operator A is then defined by

$$(63) \quad A(x) = \rho(|x|)_{20} x \quad \text{for } x \in \mathbb{R}^2.$$

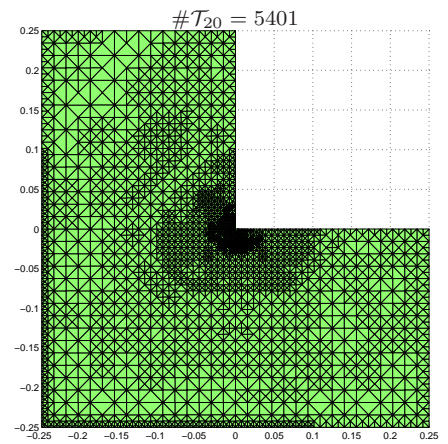
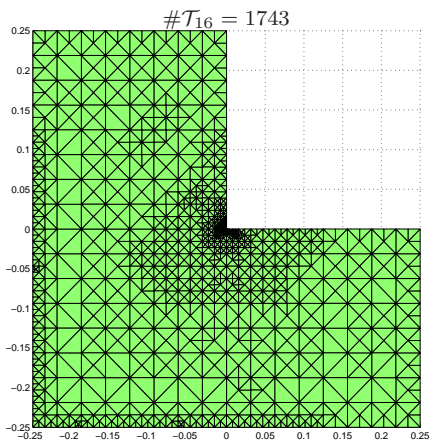
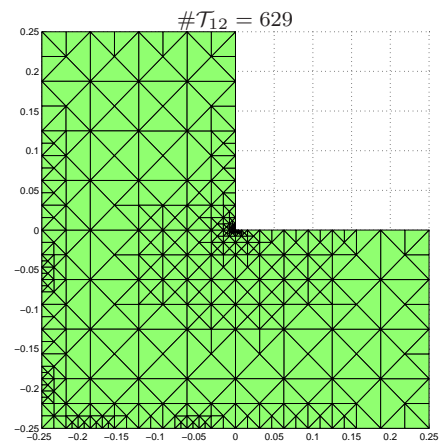
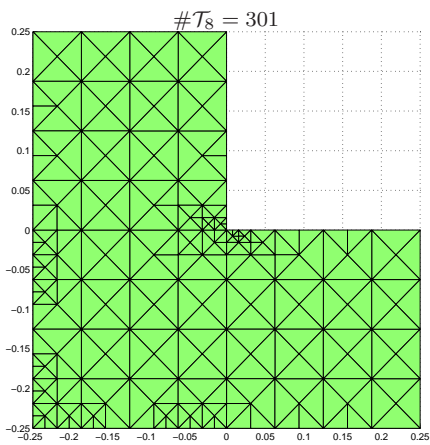
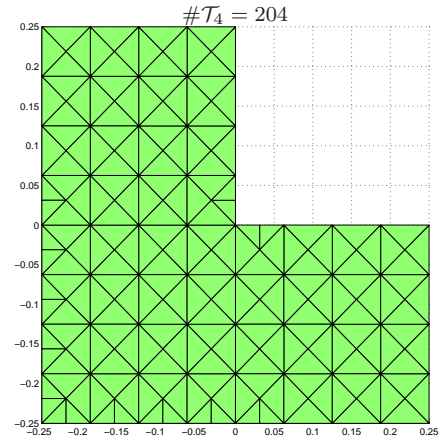
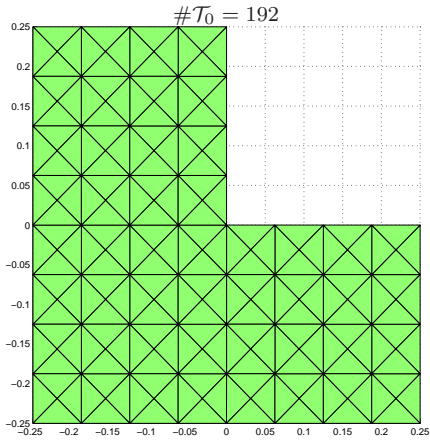


FIGURE 6. Adaptively generated meshes \mathcal{T}_ℓ in nonlinear Experiment 5.2 on the L-shaped domain.

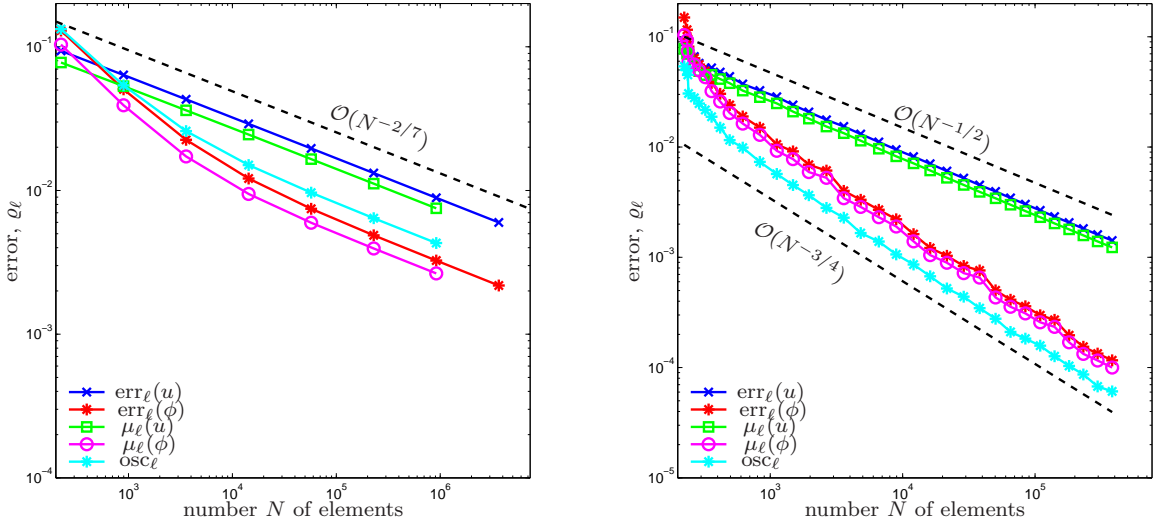


FIGURE 7. Estimators $\text{err}_\ell(u)$, $\text{err}_\ell(\phi)$, $\mu_\ell(u)$ and $\mu_\ell(\phi)$ from (58)–(59) as well as data oscillations osc_ℓ in nonlinear Experiment 5.3 on the Z-shaped domain, plotted over the number $N = \#\mathcal{T}_\ell$ of triangles for uniform (left) and adaptive mesh-refinement (right).

We stress that A is strongly monotone and Lipschitz continuous on $L^2(\Omega)^2$. We prescribe the same solution (60) as for the linear experiment from the previous section. The volume force f then reads

$$f(x, y) := -\frac{4}{27}r^{-5/3} \frac{\sin(\frac{2}{3}\varphi)}{(1 + \frac{2}{3}r^{-1/3})^2},$$

where (r, φ) are the polar coordinates of $(x, y) \in \mathbb{R}^2$ with respect to $(0, 0)$.

The nonlinear system equivalent to (24) is solved by an undamped Newton method. In our implementation, we computationally check that we are in the (quadratically convergent) asymptotic regime and stop the iteration if the Euclidean norm of the Newton residual increases. —Note that theory predicts the decay of the residual norms within the asymptotic regime.— For the initial mesh \mathcal{T}_0 , the initial guess for the Newton scheme is the constant function $\mathbf{U}_0^{(0)} \equiv 1$. For the generated meshes \mathcal{T}_ℓ , the initial guess is the preceding Galerkin approximation, i.e. $\mathbf{U}_\ell^{(0)} := \mathbf{U}_{\ell-1}$, which is prolonged to the discrete space \mathcal{X}_ℓ .

Figure 4 and 5 provide the experimental convergence results. The observations are the same as for the linear experiment in Section 5.1. Figure 6 shows some adaptively generated meshes. We observe a strong mesh-refinement towards the reentrant corner, where u^{int} is singular.

5.3. Nonlinear Problem on Z-Shaped Domain. In the final example, Ω^{int} is the Z-shaped domain, shown in Figure 1. The exact solution reads

$$(64) \quad \begin{aligned} u^{\text{int}}(x, y) &= r^{4/7} \sin(\frac{4}{7}\varphi) && \text{in } \Omega^{\text{int}}, \\ u^{\text{ext}}(x, y) &= \log \left((x + 1/8)^2 + (y + 1/8)^2 \right)^{1/2} && \text{in } \Omega^{\text{ext}}, \end{aligned}$$

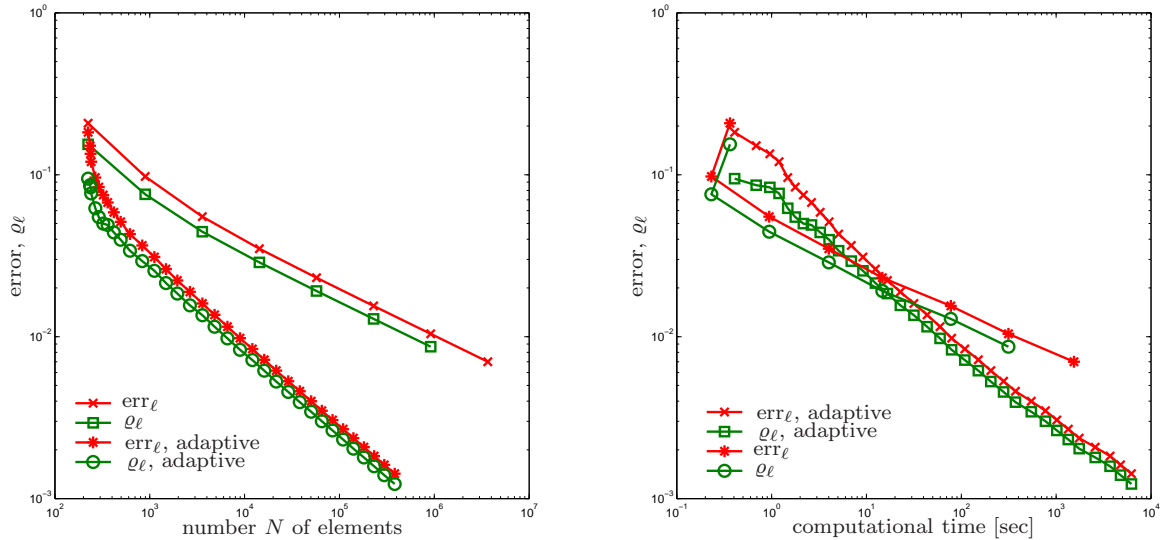


FIGURE 8. Comparison of uniform and adaptive mesh-refining in nonlinear Experiment 5.3 on the Z-shaped domain, where the error bound err_ℓ and the estimator ρ_ℓ from (61) are plotted over the number $N = \#\mathcal{T}_\ell$ of triangles (left) and over the computational time (right).

with (r, φ) being the polar coordinates of $(x, y) \in \mathbb{R}^2$. Again, u^{int} has a generic singularity at the reentrant corner. With the nonlinear operator A from Section 5.2, the right-hand side f becomes

$$-\text{div}(\rho(|\nabla u^{\text{int}}|)\nabla u^{\text{int}}) = f,$$

where

$$f(r, \varphi) := -\frac{48}{343}r^{-13/7} \frac{\sin(\frac{4}{7}\varphi)}{(1 + \frac{4}{7}r^{-3/7})^2}.$$

Figure 7 and 8 provide the experimental convergence results. As before, the observations are the same as for the linear experiment in Section 5.1. Figure 9 shows some adaptively generated meshes which show a strong mesh-refinement towards the reentrant corner.

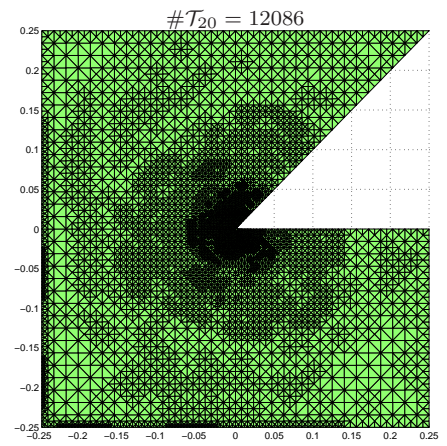
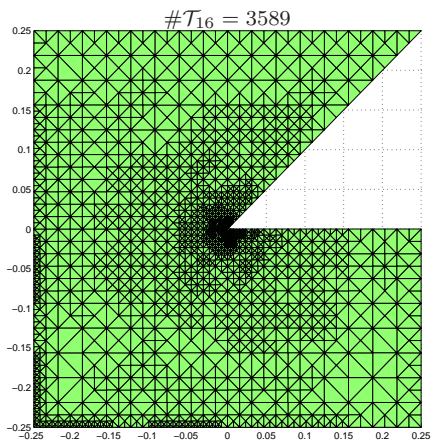
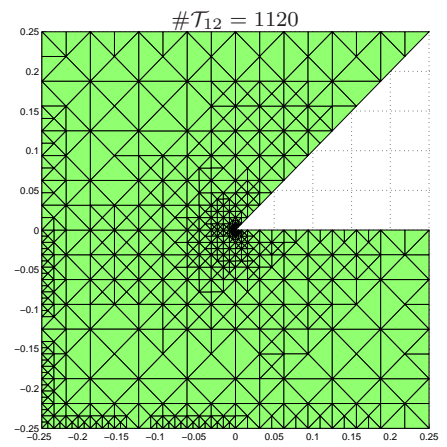
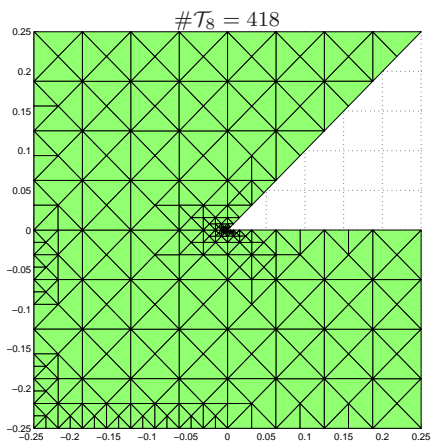
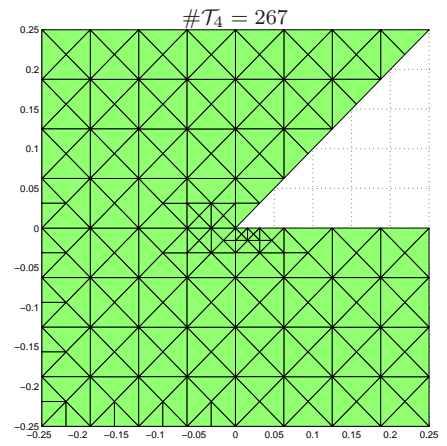
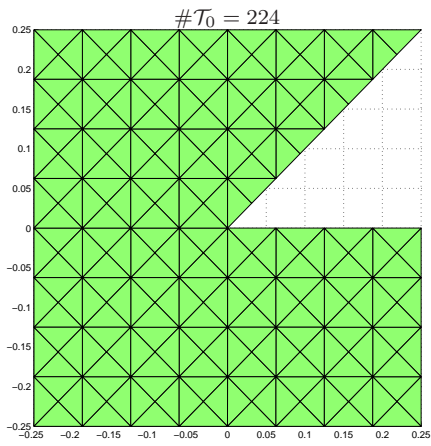


FIGURE 9. Adaptively generated meshes \mathcal{T}_ℓ in nonlinear Experiment 5.3 on the Z-shaped domain.

APPENDIX A. UNIFORM ELLIPTICITY OF DISCRETE DIRICHLET-TO-NEUMANN MAP

In [11, Section 3] it is proven that uniform ellipticity of the discrete Dirichlet-to-Neumann \mathfrak{S}_ℓ implies unique solvability of the discrete problem (18) as well as the quasi-optimality (21) of discrete solutions. Moreover, [11] prove that \mathfrak{S}_ℓ is uniformly elliptic if the mesh-width h_0 of the initial meshes \mathcal{T}_0 and \mathcal{E}_0 is sufficiently small. In this appendix, we improve this result and prove that uniform ellipticity of \mathfrak{S}_ℓ holds without further restrictions on the mesh, i.e. [11, Assumption 1] is not necessary.

To this end, we first recall the necessary definitions: Let X_ℓ be a closed subspace of $H^1(\Omega)$ and Y_ℓ be a closed subspace of $H^{-1/2}(\Gamma)$. We assume that the constant functions belong to Y_ℓ , i.e., $1 \in Y_\ell$. With the integral operators \mathfrak{V} , \mathfrak{K} , and \mathfrak{W} , the trace operator $\gamma : H^1(\Omega) \rightarrow H^{-1/2}(\Gamma)$, and the canonical inclusions

$$i_\ell : X_\ell \hookrightarrow H^1(\Omega) \quad \text{and} \quad j_\ell : Y_\ell \hookrightarrow H^{-1/2}(\Gamma),$$

we formally define the following discrete boundary integral operators

$$\begin{aligned} \mathfrak{V}_\ell &:= j_\ell^* \mathfrak{V} j_\ell : Y_\ell \rightarrow Y_\ell^*, \\ \mathfrak{K}_\ell &:= j_\ell^* \mathfrak{K} \gamma i_\ell : X_\ell \rightarrow Y_\ell^*, \\ \mathfrak{W}_\ell &:= i_\ell^* \gamma^* \mathfrak{W} \gamma i_\ell : X_\ell \rightarrow X_\ell^*. \end{aligned}$$

Moreover, we define some discrete identity

$$I_\ell = j_\ell^* \gamma i_\ell : X_\ell \rightarrow Y_\ell^*.$$

In analogy to (13), the discrete Dirichlet-to-Neumann map now reads

$$\mathfrak{S}_\ell := \mathfrak{W}_\ell + \left(\frac{1}{2} I_\ell^* - \mathfrak{K}_\ell^*\right) \mathfrak{V}_\ell^{-1} \left(\frac{1}{2} I_\ell - \mathfrak{K}_\ell\right).$$

The first elementary lemma states that \mathfrak{V}_ℓ is continuous and elliptic and that neither of these bounds depend on (X_ℓ, Y_ℓ) . In particular, \mathfrak{V}_ℓ is invertible, and \mathfrak{S}_ℓ is well-defined.

Lemma 14. *Let $C_{16}, C_{17} > 0$ denote the ellipticity constant and the operator norm of the simple-layer potential \mathfrak{V} . Then, there holds, for all $\Phi_\ell \in Y_\ell$,*

$$(65) \quad \|\mathfrak{V}_\ell \Phi_\ell\|_{Y_\ell^*} \leq C_{17} \|\Phi_\ell\|_{H^{-1/2}(\Gamma)} \quad \text{as well as} \quad \langle \mathfrak{V}_\ell \Phi_\ell, \Phi_\ell \rangle \geq C_{16} \|\Phi_\ell\|_{H^{-1/2}(\Gamma)}^2.$$

In particular, the lemma of Lax-Milgram applies and proves that \mathfrak{V}_ℓ is an isomorphism. Moreover, with $C_{18} := C_{16}/C_{17}^2$ holds

$$(66) \quad \langle Z_\ell, \mathfrak{V}_\ell^{-1} Z_\ell \rangle \geq C_{18} \|Z_\ell\|_{Y_\ell^*} \quad \text{for all } Z_\ell \in Y_\ell^*.$$

Proof. The elementary proof follows from $j_\ell \Phi_\ell = \Phi_\ell$ and $\|j_\ell^*\| = \|j_\ell\| = 1$ for the operator norms, and (66) is an immediate consequence of (65). \square

The following proposition is the main result of this appendix and obtained by bootstrapping of [11, Lemma 5].

Proposition 15. *There is a constant $C_{19} > 0$ which depends only on Ω such that for all subspaces X_ℓ of $H^1(\Omega)$ and Y_ℓ of $H^{-1/2}(\Gamma)$ with $1 \in Y_\ell$, there holds*

$$(67) \quad \langle \mathfrak{S}_\ell U_\ell, U_\ell \rangle \geq C_{19} \|U_\ell\|_{H^{1/2}(\Gamma)}^2 \quad \text{for all } U_\ell \in X_\ell.$$

Proof. We aim at proving the following claim:

$$(68) \quad \exists C_{19} > 0 \forall (X_\ell, Y_\ell)_{\ell \in \mathbb{N}} \text{ with } 1 \in Y_\ell \forall \ell \in \mathbb{N} \forall U_\ell \in X_\ell \quad \langle \mathfrak{S}_\ell U_\ell, U_\ell \rangle \geq C_{19} \|U_\ell\|_{H^{1/2}(\Gamma)}^2.$$

By choosing the constant sequence of spaces (X_ℓ, Y_ℓ) , we see that (68) implies (67). To prove (68), we argue by contradiction and assume that (68) is wrong, i.e.,

$$\forall c > 0 \exists (X_\ell, Y_\ell)_{\ell \in \mathbb{N}} \text{ with } 1 \in Y_\ell \exists \ell \in \mathbb{N} \exists U_\ell \in X_\ell \quad \langle \mathfrak{S}_\ell U_\ell, U_\ell \rangle < C_{19} \|U_\ell\|_{H^{1/2}(\Gamma)}^2.$$

For $\ell \in \mathbb{N}$ and $c = 1/\ell$, we may therefore choose some subspaces X_ℓ of $H^1(\Omega)$ and Y_ℓ of $H^{-1/2}(\Gamma)$ with $1 \in Y_\ell$ as well as some $U_\ell \in X_\ell$ such that

$$\langle \mathfrak{S}_\ell U_\ell, U_\ell \rangle < \frac{1}{\ell} \|\gamma U_\ell\|_{H^{1/2}(\Gamma)}^2$$

In particular, this yields $\gamma U_\ell \neq 0$ and hence

$$(69) \quad \langle \mathfrak{S}_\ell V_\ell, V_\ell \rangle < \frac{1}{\ell} \quad \text{with} \quad V_\ell := \frac{U_\ell}{\|\gamma U_\ell\|_{H^{1/2}(\Gamma)}} \in X_\ell \quad \text{for all } \ell \in \mathbb{N}.$$

Since $(\gamma V_\ell)_{n \in \mathbb{N}}$ is bounded in $H^{1/2}(\Gamma)$, we may assume —without loss of generality— that there holds weak convergence

$$(70) \quad \gamma V_\ell \rightharpoonup v \in H^{1/2}(\Gamma) \quad \text{as } \ell \rightarrow \infty.$$

In the following, we will now show that γV_ℓ converges to v even strongly in $H^{1/2}(\Gamma)$ and that $v \neq 0$ is constant.

First, the definition of \mathfrak{S}_ℓ and the ℓ -independent ellipticity of \mathfrak{Y}_ℓ^{-1} give

$$\begin{aligned} \langle \mathfrak{S}_\ell V_\ell, V_\ell \rangle &= \langle \mathfrak{W} \gamma V_\ell, \gamma V_\ell \rangle + \langle \mathfrak{Y}_\ell^{-1} (\tfrac{1}{2} I_\ell - \mathfrak{K}_\ell) V_\ell, (\tfrac{1}{2} I_\ell - \mathfrak{K}_\ell) V_\ell \rangle \\ &\geq \langle \mathfrak{W} \gamma V_\ell, \gamma V_\ell \rangle + C_{18} \|(\tfrac{1}{2} I_\ell - \mathfrak{K}_\ell) V_\ell\|_{Y_\ell^*}^2. \end{aligned}$$

Note that the hypersingular integral operator is positive semi-definite. Therefore, the right-hand side is nonnegative, and (69) proves that both terms on the right-hand side tend to zero. Note that the functional

$$H^{1/2}(\Omega) \rightarrow \mathbb{R}, u \mapsto \langle \mathfrak{W} u, u \rangle$$

is continuous and convex, whence weakly lower semicontinuous. With (70), this implies

$$\langle \mathfrak{W} v, v \rangle \leq \liminf_{\ell \rightarrow \infty} \langle \mathfrak{W} \gamma V_\ell, \gamma V_\ell \rangle = 0.$$

Consequently, the weak limit $v \in H^{1/2}(\Gamma)$ is constant. This and (70) imply

$$\frac{1}{|\Gamma|} \int_\Gamma \gamma V_\ell ds \xrightarrow{\ell \rightarrow \infty} \frac{1}{|\Gamma|} \int_\Gamma v ds = v.$$

Note that an equivalent norm on $H^{1/2}(\Gamma)$ is given by

$$\|u\|_{H^{1/2}(\Gamma)} \sim \| \|u\| := \left(\langle \mathfrak{W} u, u \rangle + \left| \int_\Gamma u ds \right|^2 \right)^{1/2} \quad \text{for } u \in H^{1/2}(\Gamma).$$

We now define

$$w_\ell := \gamma V_\ell - \frac{1}{|\Gamma|} \int_\Gamma \gamma V_\ell ds.$$

By definition, there holds

$$\|w_\ell\|^2 = \langle \mathfrak{W}w_\ell, w_\ell \rangle = \langle \mathfrak{W}\gamma V_\ell, \gamma V_\ell \rangle \xrightarrow{\ell \rightarrow \infty} 0,$$

i.e. there holds strong convergence $w_\ell \rightarrow 0 \in H^{1/2}(\Gamma)$. Consequently, we now obtain

$$\|\gamma V_\ell - v\|_{H^{1/2}(\Gamma)} \leq \|w_\ell\|_{H^{1/2}(\Gamma)} + \left| \frac{1}{|\Gamma|} \gamma V_\ell ds - v \right| \xrightarrow{\ell \rightarrow \infty} 0,$$

i.e. we have proven that γV_ℓ converges strongly to the constant v in $H^{1/2}(\Gamma)$. In particular, the norm convergence yields

$$\|v\|_{H^{1/2}(\Gamma)} = \lim_{\ell \rightarrow \infty} \|\gamma V_\ell\|_{H^{1/2}(\Gamma)} = 1,$$

i.e. the limit of γV_ℓ is a constant $v \neq 0$.

Since v is constant, there holds $\mathfrak{K}v = -v/2$, whence

$$0 \neq v \langle 1, 1 \rangle = \lim_{\ell \rightarrow \infty} \langle j_\ell 1, (\frac{1}{2} - \mathfrak{K})\gamma V_\ell \rangle = \lim_{\ell \rightarrow \infty} \langle 1, (\frac{1}{2} I_\ell - \mathfrak{K}_\ell)V_\ell \rangle,$$

where we have used that $1 \in Y_\ell$. However, we have already observed above that

$$\langle 1, (\frac{1}{2} I_\ell - \mathfrak{K}_\ell)V_\ell \rangle \leq \|1\|_{H^{-1/2}(\Gamma)} \|(\frac{1}{2} I_\ell - \mathfrak{K}_\ell)V_\ell\|_{Y_\ell^*} \xrightarrow{\ell \rightarrow \infty} 0.$$

This contradiction concludes the proof. \square

REFERENCES

- [1] M. AINSWORTH, J.T. ODEN: *A posteriori error estimation in finite element analysis*, Wiley-Interscience [John Wiley & Sons], New-York, 2000.
- [2] M. AURADA, M. EBNER, S. FERRAZ-LEITE, M. MAYR, P. GOLDENITS, M. KARKULIK, D. PRAETORIUS: *HILBERT — A MATLAB implementation of adaptive BEM*, ASC Report **44/2009**, Institute for Analysis and Scientific Computing, Vienna University of Technology, Wien, 2009, software download at <http://www.asc.tuwien.ac.at/abem/hilbert/>
- [3] M. AURADA, S. FERRAZ-LEITE, D. PRAETORIUS: *Estimator reduction and convergence of adaptive FEM and BEM*, ASC Report **27/2009**, Institute for Analysis and Scientific Computing, Vienna University of Technology, Wien 2009.
- [4] M. AURADA, P. GOLDENITS, D. PRAETORIUS: *Convergence of data perturbed adaptive boundary element methods*, ASC Report **40/2009**, Institute for Analysis and Scientific Computing, Vienna University of Technology, Wien 2009.
- [5] R. BANK: *Hierarchical bases and the finite element method*, Acta Numerica **5** (1996), 1–45.
- [6] C. CARSTENSEN: *An a posteriori error estimate for a first-kind integral equation*, Math. Comp. **66** (1997), 139–155.
- [7] C. CARSTENSEN, D. PRAETORIUS: *Averaging techniques for the effective numerical solution of Symm’s integral equation of the first kind*, SIAM J. Sci. Comput. **27** (2006), 1226–1260.
- [8] C. CARSTENSEN, D. PRAETORIUS: *Averaging techniques for the a posteriori BEM error control for a hypersingular integral Equation in two dimensions*, SIAM J. Sci. Comput. **29** (2007), 782–810.
- [9] C. CARSTENSEN, D. PRAETORIUS: *Averaging techniques for a posteriori error control in finite element and boundary element analysis*, in: Boundary Element Analysis: Mathematical Aspects and Applications (M. Schanz, O. Steinbach eds.), Springer Lect. Notes Appl. Comput. Mech. **29** (2007), 29–59.
- [10] C. CARSTENSEN, D. PRAETORIUS: *Convergence of adaptive boundary element methods*, ASC Report **15/2009**, Institute for Analysis and Scientific Computing, Vienna University of Technology, Wien 2009.
- [11] C. CARSTENSEN, E. STEPHAN: *Adaptive coupling of boundary elements and finite elements*, Math. Model. Numer. Anal. **29** (1995), 779–817.
- [12] M. COSTABEL: *A symmetric method for the coupling of finite elements and boundary elements*, in: The Mathematics of Finite Elements and Applications IV, MAFELAP 1987, (J. Whiteman ed.), Academic Press, London, 1988, 281–288.

- [13] P. Deuffhard, P. Leinen, H. Yserentant, *Concepts of an adaptive hierarchical finite element code*, IMPACT Comput. in. Sci. and Eng. **1** (1989), 3–35.
- [14] W. DÖRFLER: *A convergent adaptive algorithm for Poisson’s equation*, SIAM J. Numer. Anal. **33** (1996), 1106–1124.
- [15] C. ERATH, S. FERRAZ-LEITE, S. FUNKEN, D. PRAETORIUS: *Energy norm based a posteriori error estimation for boundary element methods in two dimensions*, Appl. Numer. Math. **59** (2009), 2713–2734.
- [16] C. ERATH, S. FUNKEN, P. GOLDENITS, D. PRAETORIUS: *Simple error estimators for the Galerkin BEM for some hypersingular integral equation in 2D*, ASC Report **20/2009**, Institute for Analysis and Scientific Computing, Vienna University of Technology, Wien 2009.
- [17] S. FERRAZ-LEITE, C. ORTNER, D. PRAETORIUS: *Convergence of simple adaptive Galerkin schemes based on $h - h/2$ error estimators*, ASC Report **06/2009**, Institute for Analysis and Scientific Computing, Vienna University of Technology, Wien 2009.
- [18] S. FERRAZ-LEITE, D. PRAETORIUS: *Simple a posteriori error estimators for the h-version of the boundary element method*, Computing **83** (2008), 135–162.
- [19] I. GRAHAM, W. HACKBUSCH, S. SAUTER: *Finite elements on degenerate meshes: Inverse-type inequalities and applications*, IMA J. Numer. Anal. **25** (2005), 379–407.
- [20] E. HAIRER, S. NØRSETT, G. WANNER: *Solving ordinary differential equations I. Nonstiff problems*, Springer, New York, 1987.
- [21] M. MAISCHAK, P. MUND, E. STEPHAN: *Adaptive multilevel BEM for acoustic scattering*, Comput. Methods Appl. Mech. Eng. **150** (2001), 351–367.
- [22] W. MCLEAN: *Strongly elliptic systems and boundary integral equations*, Cambridge University Press, Cambridge, 2000.
- [23] P. MORIN, K. SIEBERT, A. VEESER: *A Basic Convergence Result for Conforming Adaptive Finite Elements*, Math. Models Methods Appl. Sci. **18** (2008), 707–737.
- [24] P. MUND, E. STEPHAN: *An additive two-level method for the coupling of nonlinear FEM-BEM equations*, SIAM J. Numer. Anal. **36** (1999), 1001–1021.
- [25] P. MUND, E. STEPHAN, J. WEISSE: *Two-level methods for the single layer potential in \mathbb{R}^3* , Computing **60** (1998), 243–266.
- [26] S. RJASANOV, O. STEINBACH: *The fast solution of boundary integral equations*, Springer, New York, 2007.
- [27] S. SAUTER, C. SCHWAB: *Randelementmethoden: Analyse, Numerik und Implementierung schneller Algorithmen*, Teubner Verlag, Wiesbaden, 2004.
- [28] O. STEINBACH: *Numerical approximation methods for elliptic boundary value problems: Finite and boundary elements*, Springer, New York, 2008.
- [29] R. VERFÜRTH: *A review of a posteriori error estimation and adaptive mesh-refinement techniques*, Teubner, Stuttgart, 1996.

INSTITUTE FOR ANALYSIS AND SCIENTIFIC COMPUTING, VIENNA UNIVERSITY OF TECHNOLOGY, WIEDNER HAUPTSTRASSE 8-10, A-1040 WIEN, AUSTRIA

E-mail address: {Markus.Aurada,Michael.Feischl}@tuwien.ac.at

E-mail address: Dirk.Praetorius@tuwien.ac.at (corresponding author)